# Energy, Delay, and Outage Analysis of a Buffer-Aided Three-Node Network Relying on Opportunistic Routing

Chen Dong, Lie-Liang Yang, *Senior Member, IEEE*, Jing Zuo, Soon Xin Ng, *Senior Member, IEEE*, and Lajos Hanzo, *Fellow, IEEE*

***Abstract*—In this contribution, we propose and study a buffer-aided opportunistic routing (BOR) scheme, which combines the benefits of both opportunistic routing and multihop diversity (MHD) aided transmissions. It was conceived for a buffer-aided three-node network (B3NN) composed of a source node (SN), a buffer-aided relay node (RN) and a destination node (DN). In this network, there are three channels namely the SN-RN, RN-DN and SN-DN channels. The key motivation is that we are aiming for activating the specific channels requiring a recuded energy dissipation. In order to study this problem, a three-dimensional (3D) transmission activation probability space (TAPS) is proposed, which is divided into four regions representing each of the three channels plus an outage region. In a specific time slot (TS), the instantaneous channel fading values may be directly mapped to a specific point in this 3D channel space. The BOR scheme then relies on the position of this point to select the most appropriate channel for its transmission. Both the energy dissipation and the outage probability (OP) are investigated for transmission in this network. The results show that when the system is operated at a normalized throughput of 0.4 packet/TS, the energy dissipation was reduced by 24.8% to 77.6% compared to three different benchmark schemes. Alternatively, our technique is capable of reducing the OP by 89.6% when compared to conventional opportunistic routing. As in all buffer-aided system, the performance improved with the cost of higher packet delay, which is also studied.**

***Index Terms*—Cooperative communication, opportunistic routing, buffer, energy consumption, energy dissipation, channel space.**

## I. Introduction

MITIGATING the energy dissipation of a relay-aided wireless communication system is still an open problem at the time of writing. Employing a relay between the source node (SN) and the destination node (DN) is one of the most basic methods that can be used for mitigating energy dissipation. In this three-node relaying system, it is traditionally assumed that a packet is transmitted from the SN to the DN via the relay node (RN) sequentially. For convenience of description, we refer to this as "*the conventional three-nodes transmission scheme*" in our forthcoming discourse. This transmission scheme results in a range of advantages over conventional single-hop communications. These advantages may include an extended coverage area, an improved link performance and high-flexibility network planning, etc. [1]–[7]. However, this transmission scheme has a limited diversity order and a limited throughput. Let us discuss these drawbacks to conceive possible solutions.

The first drawback of conventional transmission is that the bit error ratio (BER)/outage performance cannot benefit from the maximum achievable diversity order, because no link prioritization scheme invoked, given that the channel activated at a specific time instant is predefined, regardless of its instantaneous channel quality (CQ). To improve the achievable performance of relaying systems, novel signalling schemes have been proposed [3], [5], [8], which require the nodes to have a store-and-wait capability. Additionally, in our previous contributions [9]–[11], we proposed a buffer-aided transmission scheme, namely the multihop diversity (MHD) transmission philosophically, which relies on temporarily storing the received packets and on activating the specific channel having the highest instantaneous SNR. Both our simulation results and theoretical analysis demonstrated that MHD transmissions are capable of achieving a substantial selection diversity gain. Recently, a relay-selection scheme was proposed in [12], while full-duplex relaying was discussed in [13]. The system model is the same as in [13], which was also considered in combination with cognitive radio [14], AF relaying [15] and physical layer security [16]. As a further advance, adaptive link selection was proposed in [17]. More recently, the performance of a two-hop buffer-aided link relying on BICM-OFDM aided relaying was analyzed in [18].

The second drawback of conventional relaying is its limited throughput, since the effective transmission duration of a specific hop in a two-hop link is halved compared to classic direct transmission [19]. More specifically, if the direct transmission has a throughput of 1 bit/s/Hz, the single-hop throughput of the two-hop system should be at least 2 bits/s/Hz for achieving the same throughput, which is a challenge in most practical cases [19]. However, Opportunistic Routing (OR) [20]–[23]

Manuscript received March 18, 2014; revised July 28, 2014, November 30, 2014, and January 19, 2015; accepted January 19, 2015. Date of publication February 4, 2015; date of current version March 13, 2015. The financial support of the RC-UK under the auspices of the India-UK Advanced Technology Centre, the support of European Research Council's Advanced Fellow Grant, the support of the EU's Concerto project and the UK/China scholarships for excellence programme is gratefully acknowledged. This paper have presented in part as "Energy-efficient buffer-aided relaying relying on non-linear channel probability space division," at the IEEE Wireless Communications and Networking Conference, Istanbul, Turkey, April 2014. The editor coordinating the review of this paper and approving it for publication was J. Yuan.

The authors are with School of ECS, University of Southampton, Southampton SO17 1BJ, U.K. (e-mail: cd2g09@ecs.soton.ac.uk; lly@ecs.soton.ac.uk; jz08r@ecs.soton.ac.uk; sxn@ecs.soton.ac.uk; lh@ecs.soton.ac.uk; http://www-mobile.ecs.soton.ac.uk).

Color versions of one or more of the figures in this paper are available online at http://ieeexplore.ieee.org.

Digital Object Identifier 10.1109/TCOMM.2015.2396512

was shown to be capable of significantly enhancing the system's throughput in relay-aided wireless transmission. For example, Liu *et al.* [21] illustrated that OR substantially increases both the transmission reliability and the throughput by exploiting the broadcast nature of the wireless medium, where all transmissions can be overheard by multiple neighbours. Biswas and Morris [20] proposed an extremely opportunistic routing (ExOR) scheme, which relied on the expected end-to-end transmission delay as the metric used for deciding on the priority order of selecting a RN from the potential forwarder set. The proposed routing regime intrinsically amalgamated the routing protocol and the medium access control (MAC) protocol for the sake of increasing the attainable throughput of multi-hop wireless networks. Their solution [20] also exploited the less reliable long-distance SN-DN links, which would have been ignored by traditional routing protocols. Zeng *et al.* [22] proposed multi-rate OR by incorporating rate-adaptation into their candidate-selection algorithm, which was shown to achieve a higher throughput and lower delay than the corresponding traditional single-rate routing and its opportunistic single-rate routing counterpart. Moreover, in our previous paper [23], we proposed an energy-efficient cross-layer aided opportunistic routing for ad hoc networks, which formulated both the normalized energy dissipation as well as the end-to-end throughput and theoretically analyzed their performances. The simulation results demonstrated that the proposed OR algorithm has a lower normalized energy dissipation and higher end-to-end throughput than the traditional multi-hop routing algorithm.

The motivation behind this paper is to combine the advantages of buffer-aided transmission with the added benefits of opportunistic routing. In the three-node network, we assumed that the RN is capable of storing a maximum of $B$ packets and the SN can transmit its packets to the DN either directly or indirectly via a RN. Without loss of generality, let us consider the scenario, where the SN-RN distance is smaller than the RN-DN distance. Even though the SN-RN distance may be different from the RN-DN distance, the probability of either of those two hops being selected should be the same, otherwise the system becomes unstable, which results in a buffer-overflow at the RN. To solve this problem, a new channel selection scheme relying on both buffer-aided transmissions and on opportunistic routing is proposed.

The key problem of this topic can be generally described as the optimization problem formulated as

$$\begin{aligned} \max \quad & \text{metric, e.g. capacity or throughput} \\ & \text{or } 1/\text{energy dissipation, etc} && (1) \\ s.t. \quad & \text{input packet} = \text{output packet for every RN} && (2) \\ & \text{Buffer limit} && (3) \\ & \text{Outage (Received SNR) limit.} && (4) \end{aligned}$$

Constraint (2) is the "main constraint" in our paper. The "Buffer limit" of (3) may be removed when we discuss the ultimate performance bound associated with an infinite buffer. Moreover, (4) may be removed when considering the achievable capacity. The above formulation is a typical optimization problem, which may be solved by applying queuing theory and Lagrange multiplier [24]. However, a different low complexity method is proposed in this paper.

There are three channels constituted by the SN-RN, SN-DN, and RN-DN links, which form a 3D transmission activation probability space (TAPS), where the TAPS is divided into four regions representing the above-mentioned three channels and the outage region. In a specific time slot, the instantaneous fading values may be directly mapped to a specific point in this 3D TAPS. The buffer-aided opportunistic routing (BOR) scheme uses this point for selecting the most appropriate channel for its next transmission. After investigating this new channel selection scheme, the end-to-end energy dissipation, OP, the position of the RN as well as the packet delay are studied. We will demonstrate that a significant energy dissipation-reduction can be achieved in comparison to the benchmark scheme. Furthermore, a meritorious MAC layer protocol is proposed for disseminating the global channel quality knowledge and the buffer-fullness (BF) of the RN.

The contributions of this paper are summarized as follows.

1. *The concept of transmission activation probability space (TAPS) and its non-linear partitioning in three nodes network is proposed, which extends the concept of classic selection combining (SC).*[1] *The three channels form a three-dimensional TAPS, which is divided into four regions, each representing one of the three channels plus an outage region. The boundary of each region is analyzed.*
2. *The end-to-end normalized energy dissipation, the system's OP and the distribution of packet delay are studied in the context of specific buffer sizes.*

The remainder of this paper is organized as follows. Section II present our system model. Then Section III to Section IV detail the concept of TAPS and its partitioning. Section V and Section VI analyzes the distribution of packet delay, exact OP and exact end-to-end Packet-Energy-Dissipation with a specific buffer size. In Section VII, we provide our numerical and simulation results. Finally, our conclusions are offered in Section VIII.

## II. System Model

Our system model is portrayed in the next three sections related to buffering, the physical layer and the transmission scheme.

### A. Buffering at the RN

Our three-node network considered in this contribution is shown in Fig. 1, which consists of a SN, a buffer-aided RN and a DN. The distances between corresponding pairs of nodes are $d_{SR}$, $d_{SD}$, and $d_{RD}$. We assume that the RN is capable of storing a maximum of $B$ packets and that the classic Decode-and-Forward protocol [25] is employed for relaying the signals.

[1] Conventionally, the SC activates the channel with the largest SNR. In the transmission activation probability space, the boundary of different region is a line or the projections of a line. For example, if there are two channels forming a plane, the boundary is a line from origin. Especially, if the two channels are identical, the boundary is a line with slope one $(y = x)$.

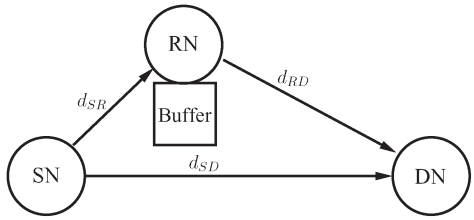


Fig. 1. System model for a buffer-aided three-node network, where SN sends messages to DN via RN, directly or indirectly.

Finally, each node is capable of adjusting its transmit power between zero and the maximum transmit power $P_{max}$.

### B. Physical Layer

In this paper, we assume that the receiver is capable of perfectly decoding the transmitted packet, when the receive SNR is higher than a specific threshold $\gamma_{T_h}$, because a sharp SNR-BER cliff for near-capacity coding (e.g., LDPC, Turbo). Based on this assumption and on the knowledge of the instantaneous channel quality, the transmitter adjusts its transmit power for ensuring that the required SNR of $\gamma_{T_h}$ is achieved at the receiver. Hence, the transmit power required is inversely proportional to the instantaneous channel quality.

We assume that the signals are transmitted on the basis of TSs having a duration of $T$ seconds. In addition to the propagation pathloss, the channels are assumed to experience independent block-based flat Rayleigh fading, where the complex-valued fading envelope of a hop remains constant within a TS, but it is independently faded for different TSs, for example by using frequency hopping. The pathloss is assumed to obey the negative exponential law of $d^{-\alpha}$, where $\alpha$ is the pathloss exponent having a value between 2 and 6. It is also assumed that the instantaneous channel quality of TS $t$ between each node pairs is denoted by $\gamma_{SR}$, $\gamma_{SD}$, and $\gamma_{RD}$. The instantaneous transmit power $\mathcal{E}_{SD}$, $\mathcal{E}_{RD}$, or $\mathcal{E}_{RD}$ of each node can then be calculated with the aid of $\kappa = 9.895 \times 10^{-05}$ and the noise power for $N = 10^{-14}$ W which corresponds to a receiver sensitivity of $-110$ dBm. An example of calculating $\mathcal{E}_{SD}$ is given by

$$\mathcal{E}_{SD} = \frac{\gamma_{T_h}}{\gamma_{SD}} \frac{d_{SD}^{\alpha} N}{\kappa}, \ \mathcal{E}_{SD} \leq P_{max}. \tag{5}$$

An outage will occur, when the receive SNR is lower than $\gamma_{T_h}$ despite using the maximum transmission power $P_{max}$, therefore we have $P_{max} = \frac{\gamma_{T_h}}{\gamma_{SD}^{out}} \frac{d_{SD}^{\alpha} N}{\kappa} = \frac{\gamma_{T_h}}{\gamma_{SR}^{out}} \frac{d_{SR}^{\alpha} N}{\kappa} = \frac{\gamma_{T_h}}{\gamma_{RD}^{out}} \frac{d_{RD}^{\alpha} N}{\kappa}$, where $\gamma_{SD}^{out}$, $\gamma_{SR}^{out}$, and $\gamma_{RD}^{out}$ are the outage thresholds of the corresponding channel.

### C. Transmission Scheme

The "action" diagram of Fig. 2 relies on two stages. The first stage is the system analysis, which is carried out before any real data transmission. Based on all the assumptions and on the independent parameters, all dependent parameters to be detailed later, including the key parameters of $\bar{\mathcal{E}}_{SR}$, $\bar{\mathcal{E}}_{RD}$, and $E_{ffe}$ may be calculated, leading to our theoretical performance results. In the second stage, simulations are carried out with the aid of all the parameters used in the first stage. The buffer-aided three-node network's (B3NN) MAC layer protocol used in the second stage will be detailed in Appendix A, which activates a single link during any TS. Again, our flow-chart-like action diagram is shown in Fig. 2. A packet will be transmitted from the SN to DN either directly or indirectly. Note that if no packets are stored in the RN, the RN-DN channel must not be activated. By contrast, if the buffer at the RN is full, the SN-RN channel must not be activated. Our studies are based on the following assumptions:

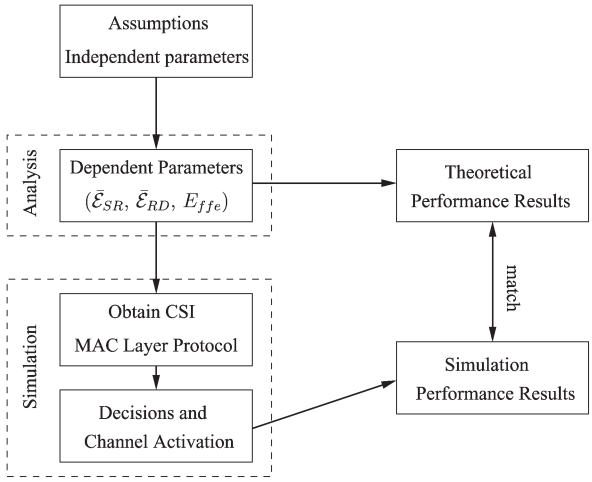


Fig. 2. The "action" diagram of this paper. During the analysis stage of this diagram, based on all the assumptions and on the independent parameters, all dependent parameters, including the key parameters of $\bar{\mathcal{E}}_{SR}$, $\bar{\mathcal{E}}_{RD}$, and $E_{ffe}$ may be calculated, leading to our theoretical performance results. During the second stage, simulations are carried out with the aid of all the parameters used in the first stage. The buffer-aided three-node network's (B3NN) MAC layer protocol used in the second stage activates a single channel during any TS. Finally, it will be shown that the theoretical and simulation results match each other well.

- The SN always has packets to send, which hence facilitates for the B3NN to operate in its steady state.
- Both the SN and DN are capable of storing an infinite number of packets. By contrast, the RN can only store a maximum of $B$ packets.
- Based on our assumptions, only a single packet is transmitted, when a channel is activated.
- The channels are assumed to be reciprocal.
- The fading processes of the three channels are independent. The fading envelope of a given hop remains constant within a packet's duration, but it is independently faded from one packet to another.
- Each node accurately adjusts its transmission power to achieve the required received SNR of $\gamma_{T_h}$.
- In each TS, only a single packet is transmitted, when the corresponding link is activated.
- Our B3NN protocol provides every node with the global channel quality and Buffer Fullness knowledge of the RNs within a given TS. All the operations of the B3NN protocol are assumed to have been carried out without a delay and without errors.

A MAC protocol conceived for controlling the operations of our B3NN is proposed in Appendix A.

## III. The Energy Dissipation Expressions

In this section, we stipulate our idealized simplifying assumptions and propose a novel node-activation scheme.

### A. Idealized Simplifying Assumptions

Our main assumption is that the average number of packets conveyed from SN to RN should be the same as those transmitted from RN to DN, which implies that the SN-RN channel and RN-DN channel should have the same probability of being activated. This assumption is automatically satisfied, when we have $d_{SR} = d_{RD}$ and when both the SN-RN and the RN-DN channel experience the same type of fading, since we have identical channel conditions in both hops. For the sake of simplicity, our node-selection scheme is highlighted in the next subsection by ignoring this assumption.

### B. Node-Activation When $d_{SR} = d_{RD}$

Our goal is to activate that particular transmitter, which mitigates the expected end-to-end Packet-Energy-Dissipation (PED) based on the knowledge of the instantaneous SNR. Since we have only three channels in the system, their PED is discussed one by one below.

1) When the SN-DN channel is activated, the end-to-end PED ($\mathcal{E}_{SD}$) is given by (5).
2) When the SN-RN channel is activated, the total PED of the SN-RN-DN route becomes the sum of the PED in each hop. However, the PED of the SN-RN hop ($\mathcal{E}_{SR}$) and that of the RN-DN hop ($\mathcal{E}_{RD}$) take place in two different time slots (TSs). Although $\mathcal{E}_{SR}$ may be known based on the current channel condition, $\mathcal{E}_{RD}$ of the RN-DN hop remains unknown in the current TS. Therefore, we use the expected PED $\bar{\mathcal{E}}_{RD}$ for estimating $\mathcal{E}_{RD}$. Hence, when the SN-RN channel is activate in TS $t$, the expected end-to-end PED becomes:

$$\mathcal{E}_{SR-\overline{RD}} = \frac{\gamma_{T_h}}{\gamma_{SR}} \frac{d_{SR}^{\alpha} N}{\kappa} + \bar{\mathcal{E}}_{RD}. \tag{6}$$

3) When the RN-DN channel is activated in TS $t$, the expected end-to-end PED is:

$$\mathcal{E}_{\overline{SR}-RD} = \bar{\mathcal{E}}_{SR} + \frac{\gamma_{T_h}}{\gamma_{RD}} \frac{d_{RD}^{\alpha} N}{\kappa}. \tag{7}$$

Finally, in each TS, the system activates that particular channel, which mitigates the expected end-to-end PED, as formulated in:

$$\mathcal{E} = \min\{\mathcal{E}_{SD}, \mathcal{E}_{SR-\overline{RD}}, \mathcal{E}_{\overline{SR}-RD}\}. \tag{8}$$

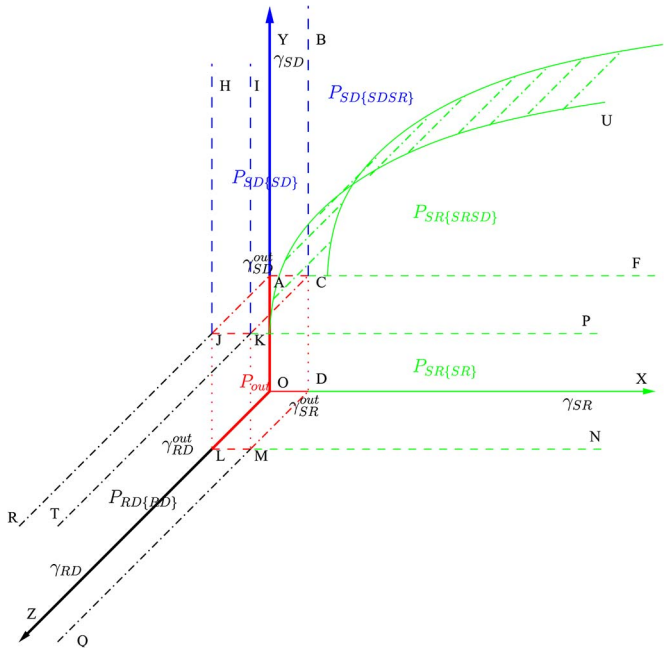


Fig. 3. The transmission activation probability space (TAPS) is divided by the outage SNR-thresholds into 8 regions. $P_{out}$ is the outage probability of the system, while $P_{SR\{SR\}}$, $P_{RD\{RD\}}$, and $P_{SD\{SD\}}$ represent the probability that only the SN-RN, the RN-DN or the SN-DN channel is available, respectively.

### C. Node-Activation When $d_{SR} \neq d_{RD}$

The previous subsection discussed both the node-activation and the PED associated with $d_{SR} = d_{RD}$, albeit in practice the RN is rarely expected in the middle. In the realistic scenario of $d_{SR} \neq d_{RD}$ the node-activation regime has to be modified, which implies that the PED is increased. Our objective is to mitigate the expected end-to-end PED. As a first step, we formulate the concept of transmission activation probability space (TAPS) in the next section. The performance bounds are analyzed throughout Sections IV under the assumption of an infinite buffer size, while in Section V and Section VI the performance results relying on a finite buffer are provided. Note that the following method is also applicable to the case of $d_{SR} = d_{RD}$.

## IV. The Concept of Transmission Activation Probability Space and Its Partitioning

In this section, the concept of TAPS is proposed first. Then, the careful partitioning of the TAPS is discussed with the objective of ensuring that on average SN-RN channel and RN-DN channel have the same probability of transmission.

### A. The Concept of Transmission Activation Probability Space

As seen from Fig. 3, the TAPS is divided into 8 subspaces based on the reception thresholds of the three channels. The following discussion will consider each of them.

Again, a three-node network is considered, where a packet can be transmitted from SN to DN both directly or indirectly via the RN. Based on Fig. 1 and on the operational principles described in Section II-C, we can now infer that if the RN has a buffer of size of $B$ packets, the following events may

TABLE I
THE POSITIONS OF THE 8 SUBSPACES

| Number | Subspace Vertex in Fig. 3 | Conditions | Candidates |
|---|---|---|---|
| 1 | ACDOLMKJ | $\gamma_{SR} < \gamma_{SR}^{out}$, $\gamma_{RD} < \gamma_{RD}^{out}$ , $\gamma_{SD} < \gamma_{SD}^{out}$ | Outage |
| 2 | FXNPKMDC | $\gamma_{SR} \geq \gamma_{SR}^{out}$, $\gamma_{RD} < \gamma_{RD}^{out}$ , $\gamma_{SD} < \gamma_{SD}^{out}$ | only $\gamma_{SR}$ |
| 3 | TRZQMLJK | $\gamma_{SR} < \gamma_{SR}^{out}$, $\gamma_{RD} \geq \gamma_{RD}^{out}$ , $\gamma_{SD} < \gamma_{SD}^{out}$ | only $\gamma_{RD}$ |
| 4 | YBIHJKCA | $\gamma_{SR} < \gamma_{SR}^{out}$, $\gamma_{RD} < \gamma_{RD}^{out}$ , $\gamma_{SD} \geq \gamma_{SD}^{out}$ | only $\gamma_{SD}$ |
| 5 | PNMQTK | $\gamma_{SR} \geq \gamma_{SR}^{out}$, $\gamma_{RD} \geq \gamma_{RD}^{out}$ , $\gamma_{SD} < \gamma_{SD}^{out}$ | $\gamma_{SR}$, $\gamma_{RD}$ |
| 6 | PKIBCF | $\gamma_{SR} \geq \gamma_{SR}^{out}$, $\gamma_{RD} < \gamma_{RD}^{out}$ , $\gamma_{SD} \geq \gamma_{SD}^{out}$ | $\gamma_{SR}$, $\gamma_{SD}$ |
| 7 | IKTRJH | $\gamma_{SR} < \gamma_{SR}^{out}$, $\gamma_{RD} \geq \gamma_{RD}^{out}$ , $\gamma_{SD} \geq \gamma_{SD}^{out}$ | $\gamma_{SD}$, $\gamma_{RD}$ |
| 8 | KPIT | $\gamma_{SR} \geq \gamma_{SR}^{out}$, $\gamma_{RD} \geq \gamma_{RD}^{out}$ , $\gamma_{SD} \geq \gamma_{SD}^{out}$ | all three channels |

TABLE II
THE PROBABILITY AND ENERGY DISSIPATION OF THE 8 SUBSPACES

| Number | Probability | Equations | Energy Dissipation | Equations |
|---|---|---|---|---|
| 1 | $P_{out}$, | (9) | - | - |
| 2 | $P_{SR\{SR\}}$ | (10) | $\mathcal{E}_{SR\{SR\}}$ | (13) |
| 3 | $P_{RD\{RD\}}$ | (11) | $\mathcal{E}_{RD\{RD\}}$ | (14) |
| 4 | $P_{SD\{SD\}}$ | (12) | $\mathcal{E}_{SD\{SD\}}$ | (15) |
| 5 | $e^{-\gamma_{SR}^{out}} e^{-\gamma_{RD}^{out}} (1 - e^{-\gamma_{SD}^{out}})$ $=P_{SR\{SR\ RD\}} + P_{RD\{SR\ RD\}}$ | (65), (70) | $\mathcal{E}_{RD\{SR\ RD\}}$ $\mathcal{E}_{SR\{SR\ RD\}}$ | Note 1 |
| 6 | $e^{-\gamma_{SR}^{out}} (1 - e^{-\gamma_{RD}^{out}}) e^{-\gamma_{SD}^{out}}$ $=P_{SR\{SR\ SD\}} + P_{SD\{SR\ SD\}}$ | (25), (32) | $\mathcal{E}_{SD\{SR\ SD\}}$ $\mathcal{E}_{SR\{SR\ SD\}}$ | Note 1 |
| 7 | $(1 - e^{-\gamma_{SR}^{out}}) e^{-\gamma_{RD}^{out}} e^{-\gamma_{SD}^{out}}$ $=P_{RD\{RD\ SD\}} + P_{SD\{RD\ SD\}}$ | (55), (60) | $\mathcal{E}_{SD\{RD\ SD\}}$ $\mathcal{E}_{RD\{RD\ SD\}}$ | Note 1 |
| 8 | $e^{-\gamma_{SR}^{out}} e^{-\gamma_{RD}^{out}} e^{-\gamma_{SD}^{out}}$ $=P_{RD\{RD\ SD\ SR\}} + P_{SD\{RD\ SD\ SR\}}$ $+P_{SR\{RD\ SD\ SR\}}$ | (71), (72), (73) | $\mathcal{E}_{RD\{RD\ SD\ SR\}}$ $\mathcal{E}_{SD\{RD\ SD\ SR\}}$ $\mathcal{E}_{SR\{RD\ SD\ SR\}}$ | Note 1 |

Note 1: The corresponding energy dissipations may be found by the corresponding probabilities equations in the same line and (26).

occur. 1) Firstly, the buffer of a RN may be empty at some instants. In this case, this RN cannot be the transmit node, since it has no data to transmit. 2) Secondly, the buffer of a RN may be full at some instants. Then, this RN cannot be the receive node, since it cannot accept further packets. In these cases, the system has to choose a hop for transmission from a reduced set of hops, which results in an increased energy dissipation and outage probability. Therefore, our performance bounds are derived by relaxing the above-mentioned constraints, namely by assuming that the RN has an unlimited buffer size and that a node always has packets to transmit, which are discussed in Sections IV-A–IV-B3. However, even with unlimited buffer size, the system should be operated in its steady state. The average number of input and output packets should be the same at the RN, which implies that that the SN-RN channel and the RN-DN channel should have the same probability of being activated, when the system is in its steady state. If we have $d_{SR} = d_{RD}$, this constraint is automatically satisfied. However, we consider a more realistic TAPS partitioning for dealing with the scenario of $d_{SR} \neq d_{RD}$.

Assuming that there is a three-dimensional space $\mathbb{S}$, a specific point associated with the coordinates $(\gamma_{SD}\ \gamma_{SR}\ \gamma_{RD})$ in $\mathbb{S}$ represents the corresponding instantaneous channel conditions of the system, hence $\mathbb{S}$ represents the TAPS of the system. The outage SNR-threshold associated with each coordinate $\gamma_{SD}^{out}$, $\gamma_{SR}^{out}$, and $\gamma_{RD}^{out}$ dissects each coordinate into two segments, hence $\mathbb{S}$ is decomposed into $2^3 = 8$ subspaces. The vertex of each subspace, the conditions, the activated channel candidates and the probability/energy dissipation are listed in Tables I and II.

Fig. 3 shows the resultant TAPS. A system outage occurs, when none of the nodes can transmit, because we have excessively low instantaneous SNRs of $\gamma_{SR} < \gamma_{SR}^{out}$, $\gamma_{RD} < \gamma_{RD}^{out}$, and $\gamma_{SD} < \gamma_{SD}^{out}$. The outage probability is denoted by $P_{out}$ (which is represented by the cube defined by the points ACDOLMKJ in Fig. 3), yielding

$$P_{out} = \left(1 - e^{-\gamma_{SR}^{out}}\right)\left(1 - e^{-\gamma_{RD}^{out}}\right)\left(1 - e^{-\gamma_{SD}^{out}}\right). \tag{9}$$

Let $P_{SR}$, $P_{RD}$ and $P_{SD}$ represent the probability that the corresponding channel is selected. Naturally, we expect $P_{SR} + P_{RD} + P_{SD} + P_{out} = 1$. Let us introduce the notation $P_{Ch_A\{Ch_1,Ch_2\}}$, which represents the concurrent probability of 1) channel A is activated; 2) both the instantaneous fading values of channel "1" and "2" are higher than the corresponding outage threshold, in other words these channels are activation candidates. For example, $P_{SR\{SR\}}$ implies that the SR link is activated only when $\gamma_{SR}$ is higher than its corresponding threshold. Using the same logic, $P_{SR\{SR\ SD\}}$ indicates the SR hop is activated, when both $\gamma_{SR}$ and $\gamma_{SD}$ are higher than their corresponding thresholds. Finally, $P_{SR\{SR\ SD\ RD\}}$ means that the SR link is activated, when the channel quality of each hop is higher than its corresponding threshold. Naturally, we have $P_{SR} = P_{SR\{SR\}} + P_{SR\{SR\ RD\}} + P_{SR\{SR\ SD\}} + P_{SR\{SR\ RD\ SD\}}$ and the same properties are valid for $P_{RD}$ and $P_{SD}$.[2] If there is only a single instantaneous channel fading value above the corresponding outage threshold, the system will activate that particular channel. For example, $P_{SR\{SR\}}$

[2]Later, the same properties are valid for $\mathcal{E}_{SD}$, $\mathcal{E}_{SR}$, and $\mathcal{E}_{RD}$.

is the probability represented by the prism defined by the points KCDMNXFP in Fig. 3. The corresponding probabilities are

$$P_{SR\{SR\}} = P\left(\gamma_{SR} \geq \gamma_{SR}^{out}\right) P\left(\gamma_{RD} < \gamma_{RD}^{out}\right) P\left(\gamma_{SD} < \gamma_{SD}^{out}\right) = e^{-\gamma_{SR}^{out}} \left(1 - e^{-\gamma_{RD}^{out}}\right) \left(1 - e^{-\gamma_{SD}^{out}}\right), \quad (10)$$

Similarly, we have

$$P_{RD\{RD\}} = \left(1 - e^{-\gamma_{SR}^{out}}\right) e^{-\gamma_{RD}^{out}} \left(1 - e^{-\gamma_{SD}^{out}}\right), \quad (11)$$

$$P_{SD\{SD\}} = \left(1 - e^{-\gamma_{SR}^{out}}\right) \left(1 - e^{-\gamma_{RD}^{out}}\right) e^{-\gamma_{SD}^{out}}, \quad (12)$$

and the energy dissipation in corresponding regions

$$\mathcal{E}_{SR\{SR\}} = \left(1 - e^{-\gamma_{RD}^{out}}\right) \left(1 - e^{-\gamma_{SD}^{out}}\right) \times \int_{\gamma_{SR}^{out}}^{\infty} e^{-\gamma_{SR}} \frac{\gamma_{T_h}}{\gamma_{SR}} \frac{d_{SR}^{\alpha} N}{\kappa} d\gamma_{SR}, \quad (13)$$

$$\mathcal{E}_{RD\{RD\}} = \left(1 - e^{-\gamma_{SR}^{out}}\right) \left(1 - e^{-\gamma_{SD}^{out}}\right) \times \int_{\gamma_{RD}^{out}}^{\infty} e^{-\gamma_{RD}} \frac{\gamma_{T_h}}{\gamma_{RD}} \frac{d_{RD}^{\alpha} N}{\kappa} d\gamma_{RD}, \quad (14)$$

$$\mathcal{E}_{SD\{SD\}} = \left(1 - e^{-\gamma_{RD}^{out}}\right) \left(1 - e^{-\gamma_{SR}^{out}}\right) \times \int_{\gamma_{SD}^{out}}^{\infty} e^{-\gamma_{SD}} \frac{\gamma_{T_h}}{\gamma_{SD}} \frac{d_{SD}^{\alpha} N}{\kappa} d\gamma_{SD}, \quad (15)$$

where $Ei(x) = \int_{-x}^{\infty} \frac{e^{-t}}{t} dt$ [26] (8.211.1) may further simplify this expressions. Having introduced the concept of TAPS and the calculation of the probabilities of $P_{out}$, $P_{SR\{SR\}}$, $P_{RD\{RD\}}$, and $P_{SD\{SD\}}$, more complicated scenarios, such as $P_{SR\{SR\ SD\}}$ are discussed in follow.

### B. Partitioning the Transmission Activation Probability Space

In this section, we commence by introducing the energy efficiency factor $E_{ffe}$ and then the probabilities $P_{SR\{SR\ SD\}}$ as well as $P_{SD\{SR\ SD\}}$ represented by the prism defined by the points BCFPKI in Fig. 3 are explored. The associated activation process can be applied under diverse channel selection scenarios represented by this system model.

*1) The Energy Efficiency Factor $E_{ffe}$:* The channel selection associated with the region BCFPKI of Fig. 3 is further restricted by the specific conditions of $\gamma_{SR} \geq \gamma_{SR}^{out}$, $\gamma_{RD} < \gamma_{RD}^{out}$, and $\gamma_{SD} \geq \gamma_{SD}^{out}$. Explicitly, since we have $\gamma_{RD} < \gamma_{RD}^{out}$, let us find the activation boundary between the region of activating the SR or SD links in the region BCFPKI. As shown in Fig. 3, let us only discuss the projection to the surface XOY, which is shown as Fig. 4. The line OCE' of this surface in Fig. 4 represents the scenario, where the SR and SD channels have the same received SNR.

To deal with the problem of $P_{SR} > P_{RD}$, some of the regions that used to correspond to the activation of the SR hop have to be reassigned, either to the RD hop or to the SD hop. However, this adjustment imposes extra energy dissipation. Hence, the activation regions are carefully reassigned based on

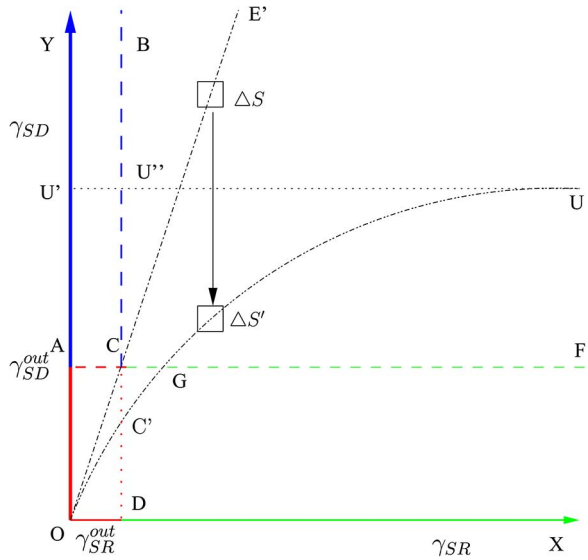


Fig. 4. A plane in TAPS which shows that the channel selection is only between SN-RN hop and SN-DN hop.

the associated energy efficiency factor $E_{ffe}$, which is defined as the extra energy dissipation divided by the reassignment probability. This process is detailed below.

Let us denote the probability of encountering a small region $\Delta S$ on the surface OCE of Fig. 4 by $p_{\Delta S}$. The coordinates of $\Delta S$ are $(\gamma_{\Delta S_{SR}}, \gamma_{\Delta S_{SD}})$. When the region $\Delta S$ belongs to the SR hop and the SR hop is activated, then the expected end-to-end energy dissipated upon encountering the region $\Delta S$ is calculated from (6), yielding

$$\mathcal{E}_{\Delta S \in SR} = p_{\Delta S} \left( \frac{\gamma_{T_h} d_{SR}^{\alpha} N}{\gamma_{\Delta S_{SR}} \kappa} + \bar{\mathcal{E}}_{RD} \right). \quad (16)$$

By contrast, when the region $\Delta S$ belongs to the SD hop and the SD hop is activated, the expected end-to-end energy dissipated upon encountering the region $\Delta S$ is calculated from (5), yielding

$$\mathcal{E}_{\Delta S \in SD} = p_{\Delta S} \left( \frac{\gamma_{T_h} d_{SD}^{\alpha} N}{\gamma_{\Delta S_{SD}} \kappa} \right). \quad (17)$$

If the region $\Delta S$ is reassigned from the SR hop to the SD hop, the extra energy dissipation becomes

$$\Delta \mathcal{E}_{\Delta S} = p_{\Delta S} \left( \frac{\gamma_{T_h} d_{SD}^{\alpha} N}{\gamma_{\Delta S_{SD}} \kappa} - \frac{\gamma_{T_h} d_{SR}^{\alpha} N}{\gamma_{\Delta S_{SR}} \kappa} - \bar{\mathcal{E}}_{RD} \right). \quad (18)$$

Hence, if we know the probability $p_{\Delta S}$ of encountering the region $\Delta S$ of Fig. 4, $E_{ffe}$ is defined as

$$E_{ffe} = \frac{\gamma_{T_h} d_{SD}^{\alpha} N}{\gamma_{\Delta S_{SD}} \kappa} - \frac{\gamma_{T_h} d_{SR}^{\alpha} N}{\gamma_{\Delta S_{SR}} \kappa} - \bar{\mathcal{E}}_{RD}. \quad (19)$$

The specific value of $E_{ffe}$ may then be determined from the equations, whilst a practical algorithm will be provided for solving these equations in Section IV-B3. In the remainder of this section, $E_{ffe}$ is considered to be a known parameter. Note that the $E_{ffe}$ may be positive or negative reflecting the boundary bended direction. As exemplified in Fig. 4 and (19), the $E_{ffe}$ is negative when $\gamma_{\Delta S_{SD}} \to \infty$. The boundary OU bends to Y-axis

and it is on the left side of $OCE'$, which means that some probability region is adjusted from SD hop to SR hop.

*2) Definition of $P_{SR\{SR\ SD\}}$ and $P_{SD\{SR\ SD\}}$:* Having introduced $E_{ffe}$, this subsection explores the boundary of two activation regions, which was formulated in (19). Explicitly, the boundary is expressed with the aid of $\gamma_{SR\{SR\ SD\}}$ and $\gamma_{SD\{SR\ SD\}}$ instead of $\gamma_{\Delta S_{SR}}$ and $\gamma_{\Delta S_{SD}}$ in (19). Upon substituting $\gamma_{SR\{SR\ SD\}}$ and $\gamma_{SD\{SR\ SD\}}$ for $\gamma_{\Delta S_{SR}}$ and $\gamma_{\Delta S_{SD}}$, we have

$$E_{ffe} = \frac{\gamma_{T_h} d_{SD}^{\alpha} N}{\gamma_{SD\{SR\ SD\}} \kappa} - \frac{\gamma_{T_h} d_{SR}^{\alpha} N}{\gamma_{SR\{SR\ SD\}} \kappa} - \bar{\mathcal{E}}_{RD} \tag{20}$$

$$\Longrightarrow \gamma_{SD\{SR\ SD\}} = \frac{\gamma_{T_h} d_{SD}^{\alpha} \kappa}{E_{ffe}\kappa + \bar{\mathcal{E}}_{RD}\kappa + \frac{\gamma_{T_h} d_{SR}^{\alpha} N}{\gamma_{SR\{SR\ SD\}}}}. \tag{21}$$

Here, $\gamma_{SR\{SR\ SD\}}$ is the independent variable and $\gamma_{SD\{SR\ SD\}}$ is the dependent variable which form the boundary "GU" in Fig. 4. A function $f_{\{x->y\}}$ is defined that $x$ is the independent variable and $y$ is the dependent variable.

$$f_{\{\gamma_{SR}->\gamma_{SD}\}}\left(\gamma_{SR\{SR\ SD\}}\right) = \frac{\gamma_{T_h} d_{SD}^{\alpha} \kappa}{E_{ffe}\kappa + \bar{\mathcal{E}}_{RD}\kappa + \frac{\gamma_{T_h} d_{SR}^{\alpha} N}{\gamma_{SR\{SR\ SD\}}}}. \tag{22}$$

Having (22), where the domain of definition for $\gamma_{SD\{SR\ SD\}}$ is $(\gamma_{SD}^{out}, \infty)$[3] (CB in Fig. 4), and hence that for $\gamma_{SR\{SR\ SD\}}$ is $(\gamma_{SR\{SR\ SD\}}^{min}, \gamma_{SR\{SR\ SD\}}^{max})$ (GF in Fig. 4), yielding

$$\gamma_{SR\{SR\ SD\}}^{min} = \max\left\{\gamma_{SR}^{out}, f_{\{SR->SD\}}^{-1}\left(\gamma_{SD}^{out}\right)\right\} \tag{23}$$

$$\gamma_{SR\{SR\ SD\}}^{max} = f_{\{SR->SD\}}^{-1}(\infty). \tag{24}$$

If $f_{\{SR->SD\}}^{-1}(\infty)$ has no positive solution,[4] we have $\gamma_{SD\{SR\ SD\}}^{max} = \infty$. A specific example of $E_{ffe} > 0$ is shown in Fig. 4, where $\gamma_{SR}^{out}$ is at point C and $f_{\{SR->SD\}}^{-1}(\gamma_{SD}^{out})$ is at point G. Hence $\gamma_{SR\{SR\ SD\}}^{min}$ is at point G, while $f_{\{SR->SD\}}^{-1}(\infty)$ has no solution, therefore, we have $\gamma_{SD\{SR\ SD\}}^{max} = \infty$. Finally, the boundary for this example between activating the two hops is the curve GU.

Assuming that we have $\mathcal{F}_1(\gamma_{SR\{\bullet\}}) = 1$, $\mathcal{F}_2(\gamma_{SR\{\bullet\}}) = \frac{\gamma_{T_h} N}{\kappa} \frac{d_{SR}^{\alpha}}{\gamma_{SR\{\bullet\}}}$ and $\mathcal{F}_3(\gamma_{SR\{\bullet\}}) = \log_2(1 + \gamma_{SR}\gamma_{h_{SR}})$, the resultant activation probability $P_{SR\{SR\ SD\}}$, the expected energy dissipation $\mathcal{E}_{SR\{SR\ SD\}}$ and the capacity $C_{SR\{SR\ SD\}}$ of the SR link (region FGU in Fig. 4) associated with the domain BCFPKI of Fig. 3 may be formulated as:

$$\begin{aligned} P_{SR\{SR\ SD\}} &= \left(1 - e^{-\gamma_{RD}^{out}}\right) \int_{\gamma_{SR\{SR\ SD\}}^{min}}^{\gamma_{SR\{SR\ SD\}}^{max}} \mathcal{F}_1\left(\gamma_{SR\{SR\ SD\}}\right) e^{-\gamma_{SR\{SR\ SD\}}} \\ &\quad \times \int_{\gamma_{SD}^{out}}^{f_{\{SR->SD\}}(\gamma_{SR\{SR\ SD\}})} e^{-\gamma_{SD\{SR\ SD\}}} \\ &\quad \times d\gamma_{SD\{SR\ SD\}} d\gamma_{SR\{SR\ SD\}}, \end{aligned} \tag{25}$$

$$\begin{aligned} \mathcal{E}_{SR\{SR\ SD\}} &= \left(1 - e^{-\gamma_{RD}^{out}}\right) \int_{\gamma_{SR\{SR\ SD\}}^{min}}^{\gamma_{SR\{SR\ SD\}}^{max}} \mathcal{F}_2\left(\gamma_{SR\{SR\ SD\}}\right) e^{-\gamma_{SR\{SR\ SD\}}} \\ &\quad \times \int_{\gamma_{SD}^{out}}^{f_{\{SR->SD\}}(\gamma_{SR\{SR\ SD\}})} e^{-\gamma_{SD\{SR\ SD\}}} \\ &\quad \times d\gamma_{SD\{SR\ SD\}} d\gamma_{SR\{SR\ SD\}}, \end{aligned} \tag{26}$$

$$\begin{aligned} C_{SR\{SR\ SD\}} &= \left(1 - e^{-\gamma_{RD}^{out}}\right) \int_{\gamma_{SR\{SR\ SD\}}^{min}}^{\gamma_{SR\{SR\ SD\}}^{max}} \mathcal{F}_3\left(\gamma_{SR\{SR\ SD\}}\right) e^{-\gamma_{SR\{SR\ SD\}}} \\ &\quad \times \int_{\gamma_{SD}^{out}}^{f_{\{SR->SD\}}(\gamma_{SR\{SR\ SD\}})} e^{-\gamma_{SD\{SR\ SD\}}} \\ &\quad \times d\gamma_{SD\{SR\ SD\}} d\gamma_{SR\{SR\ SD\}}. \end{aligned} \tag{27}$$

In the remainder of this treatise only the activation probability of the links is formulated explicitly, which may be readily extended to the energy dissipation and capacity formulas.[5]

To elaborate a little further, the relationship between $\gamma_{SR\{SR\ SD\}}$ and $\gamma_{SD\{SR\ SD\}}$ is also based on (20), which may be written as

$$\gamma_{SR\{SR\ SD\}} = \frac{\gamma_{T_h} d_{SR}^{\alpha} \kappa}{-E_{ffe}\kappa - \bar{\mathcal{E}}_{RD}\kappa + \frac{\gamma_{T_h} d_{SD}^{\alpha} N}{\gamma_{SD\{SR\ SD\}}}}. \tag{28}$$

As before, let us define a function $f_{\{SD->SR\}}(\gamma_{SD\{SR\ SD\}})$ to express (28) as

$$f_{\{SD->SR\}}\left(\gamma_{SD\{SR\ SD\}}\right) = \frac{\gamma_{T_h} d_{SR}^{\alpha} \kappa}{-E_{ffe}\kappa - \bar{\mathcal{E}}_{RD}\kappa + \frac{\gamma_{T_h} d_{SD}^{\alpha} N}{\gamma_{SD\{SR\ SD\}}}}, \tag{29}$$

where $\gamma_{SD\{SR\ SD\}}$ is the independent variable and $\gamma_{SR\{SR\ SD\}}$ is the dependent variable. The domain of definition for $\gamma_{SD\{SR\ SD\}}$ is defined as $(\gamma_{SD\{SR\ SD\}}^{min}, \gamma_{SD\{SR\ SD\}}^{max})$,[6] yielding

$$\gamma_{SD\{SR\ SD\}}^{min} = \max\left\{\gamma_{SD}^{out}, f_{\{SD->SR\}}^{-1}\left(\gamma_{SR}^{out}\right)\right\} \tag{30}$$

$$\begin{aligned} \gamma_{SD\{SR\ SD\}}^{max} &= f_{\{SD->SR\}}^{-1}(\infty) \\ \Longrightarrow \infty &= \frac{\gamma_{T_h} d_{SR}^{\alpha} \kappa}{-E_{ffe}\kappa - \bar{\mathcal{E}}_{RD}\kappa + \frac{\gamma_{T_h} d_{SD}^{\alpha} N}{\gamma_{SD\{SR\ SD\}}^{max}}} \\ \Longrightarrow \gamma_{SD\{SR\ SD\}}^{max} &= \frac{\gamma_{T_h} d_{SD}^{\alpha} N}{E_{ffe}\kappa + \bar{\mathcal{E}}_{RD}\kappa}, \end{aligned} \tag{31}$$

where $\gamma_{SD\{SR\ SD\}}^{max}$ is less than infinity. For example, in Fig. 4, $\gamma_{SD\{SR\ SD\}}^{max}$ is represented by the $U'$ point. The region above the $U'$ point (i.e., that region $UU''B$) belongs to the SD hop. The

[3]When we have $\gamma_{SD} > \gamma_{SD}^{out}$, the SD channel has a certain probability to be selected and we want to find this probability. On the other hand, if a channel has an infinite SNR, this channel will be definitely selected. It is plausible that the domain of definition of this input value is $(\gamma_{SD}^{out}, \infty)$.

[4]This principle is suitable for all functions $f_{\{\bullet\}}^{-1}(\infty)$, regardless of the sign of $E_{ffe}$.

[5]Note that, some integrals derived in this paper cannot be expressed in closed-form. However, all formulas can be simplified to a single integral. The infinite value of the channel SNR may be considered as a large finite value, such as say 10. Therefore, a finite single integral can be efficiently evaluated by commercial software, such as MATLAB, Maple and Mathematica.

[6]The domain of $\gamma_{SD}$ is $(\gamma_{SD}^{out}, \infty)$ which is CB in Fig. 3. However, it should be discussed in the context of two cases. When channel SR competes with channel SD, the range of channel SD is $(\gamma_{SD\{SR\ SD\}}^{min}, \gamma_{SD\{SR\ SD\}}^{max})$, which is CU$''$ in Fig. 3. By contrast, the range of channel SD is $(\gamma_{SD\{SR\ SD\}}^{max}, \infty)$ when no channel competes with channel SD, which is represented by U$''$B in Fig. 3.

activation probability $P_{SD\{SR\ SD\}}$ of the SD link associated with $\gamma_{SD\{SR\ SD\}}$. $P_{SD\{SR\ SD\}}$ is expressed as:

$$\begin{aligned} P_{SD\{SR\ SD\}} &= \left(1-e^{-\gamma_{RD}^{out}}\right)\int_{\gamma_{SD\{SR\ SD\}}^{min}}^{\gamma_{SD\{SR\ SD\}}^{max}} \mathcal{F}_1\left(\gamma_{SD\{SR\ SD\}}\right) e^{-\gamma_{SD\{SR\ SD\}}} \\ &\quad \times \int_{\gamma_{SR}^{out}}^{f_{\{SD->SR\}}\left(\gamma_{SD\{SR\ SD\}}\right)} e^{-\gamma_{SR\{SR\ SD\}}} \\ &\quad \times d\gamma_{SR\{SR\ SD\}} d\gamma_{SD\{SR\ SD\}} \\ &\quad + \left(1-e^{-\gamma_{RD}^{out}}\right) e^{-\gamma_{SR}^{out}} \int_{\gamma_{SD\{SR\ SD\}}^{max}}^{\infty} \mathcal{F}_1\left(\gamma_{SD\{SR\ SD\}}\right) \\ &\quad \times e^{-\gamma_{SD\{SR\ SD\}}} d\gamma_{SD\{SR\ SD\}}. \end{aligned} \tag{32}$$

By repeating the process described in the previous subsection, we may readily derive $P_{SD\{SD\ RD\}}$, $P_{RD\{SD\ RD\}}$, $P_{SR\{SR\ RD\}}$, $P_{RD\{SR\ RD\}}$, and even $P_{SD\{SD\ SR\ RD\}}$, $P_{SR\{SD\ SR\ RD\}}$ as well as $P_{RD\{SD\ SR\ RD\}}$. For the details, please see Appendix-B to D.

*3) Finding the Optimal $E_{ffe}$:* In the previous sections, we had three unknowns: $\bar{\mathcal{E}}_{SR}$, $\bar{\mathcal{E}}_{SR}$ and $E_{ffe}$. Given all the expected energy dissipations $\mathcal{E}_{\{\bullet\}}$ and all the activation probabilities $P_{\bullet\{\bullet\}}$, the three unknowns can be obtained from the following three equations:

$$\begin{aligned} \bar{\mathcal{E}}_{SR} &= \frac{\mathcal{E}_{SR}}{P_{SR}} \\ &= \frac{\mathcal{E}_{SR\{SR\}}+\mathcal{E}_{SR\{SRSD\}}+\mathcal{E}_{SR\{SRRD\}}+\mathcal{E}_{SR\{SRSDRD\}}}{P_{SR\{SR\}}+P_{SR\{SRSD\}}+P_{SR\{SRRD\}}+P_{SR\{SRSDRD\}}} \end{aligned} \tag{33}$$

$$\begin{aligned} \bar{\mathcal{E}}_{RD} &= \frac{\mathcal{E}_{RD}}{P_{RD}} \\ &= \frac{\mathcal{E}_{RD\{RD\}}+\mathcal{E}_{RD\{SRSD\}}+\mathcal{E}_{RD\{RDSD\}}+\mathcal{E}_{RD\{SRSDRD\}}}{P_{RD\{RD\}}+P_{RD\{SRSD\}}+P_{RD\{RDSD\}}+P_{RD\{SRSDRD\}}} \end{aligned} \tag{34}$$

$$P_{SR} = P_{RD}. \tag{35}$$

However, it is not practical to directly solve these integral equations. Hence, we conceive a simple algorithm for finding the solution.

The basic principle is that of employing an exhaustive search for finding the optimal $E_{ffe}$. All energy dissipations and activation probabilities as well as (33) and (34) can be evaluated for a specific $E_{ffe}$. Therefore, we search for specific $E_{ffe}$ values starting from zero and terminating when (35) is satisfied.

**Algorithm 1**: The algorithm of finding $E_{ffe}$

1 $E_{ffe} = 0$;
2 Calculate all activation probabilities and energy dissipations;
3 Update $\bar{\mathcal{E}}_{SR}$ and $\bar{\mathcal{E}}_{RD}$ based on (33) and (34);
4 **while** $P_{SR} \neq P_{RD}$ **do**
5 Increase $E_{effe}$;
6 Calculate all selection probabilities and energy dissipations;
7 Update $\bar{\mathcal{E}}_{SR}$ and $\bar{\mathcal{E}}_{RD}$ based on (33) and (34);
8 **end**

Finally, the theoretical end-to-end energy dissipation is given by the ratio of the total energy dissipation to the throughput, yielding

$$\bar{\mathcal{E}}_{SD} = \frac{\mathcal{E}_{SD}+\mathcal{E}_{SR}+\mathcal{E}_{RD}}{P_{SD}+P_{SR}}. \tag{36}$$

### C. Discussion of the General Applicability of the TAPS Concept

Recall from (1) to (4) that our problem is actually a Functional Integration problem. Generally speaking, the Functional Integration (e.g., (2)) may be translated to:

$$\begin{aligned} &\int_0^{\infty}\int_{G_1(\gamma_1)}^{\infty}\cdots\int_{G_k(\gamma_1,\cdots,\gamma_k)}^{\infty} \underbrace{\text{Metric1 } p(\gamma_1,\cdots,\gamma_{k+1})}_{\text{Inner}} \\ &\quad \times d\gamma_{k+1}d\gamma_k\cdots d\gamma_1 \\ &= \int_0^{\infty}\int_{H_1(\gamma_1)}^{\infty}\cdots\int_{H_k(\beta_1,\cdots,\beta_k)}^{\infty} \underbrace{\text{Metric2 } p(\beta_1,\cdots,\beta_{k+1})}_{\text{Inner}} \\ &\quad \times d\beta_{k+1}d\beta_k\cdots d\beta_1. \end{aligned} \tag{37}$$

Let us interpret the physical meaning of (37) one by one, where $\gamma_1,\cdots,\gamma_{k+1}$ and $\beta_1,\cdots,\beta_{k+1}$ are the instantaneous fading values of the channels in the system. The two groups of random variables may have an overlap. Furthermore, $p(\gamma_1,\cdots,\gamma_{k+1})$ and $p(\beta_1,\cdots,\beta_{k+1})$ represent the joint probability of the random variables. Next to $p(.)$, the terminology "Metric" represents the metric to be evaluated by the activated channels. For example, $\log 2(1+C_1\gamma_i)$ is the capacity of the $i$th channel, where $C_1$ is the average received SNR of the $i$th channel, which is a constant value. Another metric is exemplified by $\frac{C_2}{\gamma_i}$, which is the energy dissipation, and this is inversely proportional to the instantaneous fading value. What we want to find now are the functions $G_1, G_2, \cdots, G_k$ and $H_1, H_2, \cdots, H_k$. Generally, there is no other solution for (37) than the brute-force exhaustive search as discussed in the last paragraph of Section IV-B in [25]: "a two dimensional search over all $\lambda > 0$ and $\rho > 0$ has to be conducted or built-in root-finding functions…."

However, our specific problem exhibits particular properties: the metric (e.g., capacity) is a monotonic function of the activated channel quality. This is the key, which allows us to use the greedy algorithm. Hence, we generalized the partitioning algorithm operating on the TAPS. Note that Step 2 below represents the key step, which only considers the adjustment of the 'Inner' part explicitly marked in (37) and finally we can find $G_1,\cdots,G_k$ and $H_1,\cdots,H_k$ automatically, when the algorithm is terminated. This is a greedy algorithm, where it was sufficient to consider only the 'Inner' part of (37), which reduced the complexity imposed. By contrast, the exhaustive searching method considered the entire integral in (37).

Step 1: Find the solution of (1) without imposing the constraint (2). Algebraically, the channel having

the maximum fading envelope value of $\max\{\gamma_1,\gamma_2,\cdots,\gamma_L\}$ is activated. Geometrically, the boundary of each region in TAPS is linear. On the boundary, activating any of the associated channels has the same result, which is formulated as $Metric(\gamma_i) = Metric(\gamma_j)$.

Step 2: Relocate a small probability-cube (tile) on the boundary from one region to another adjacent region to approach the constraint (2). Geometrically, the boundary of each region is no longer a linear. Algebraically, the boundary (activation criterion) changes to $Metric(\gamma_i) = Metric(\gamma_j) + E_{ffe}$, where $E_{ffe}$ is a compensation parameter, positive or negative. The original complex problem becomes that of searching for the only adjustable parameter namely for $E_{ffe}$, which can be achieved at a modest complexity. The corresponding complexity increases quadratically with the number of channels, since the number of channel pair increases quadratically.

Step 3: The adjustment process commences from $E_{ffe} = 0$ and terminates when the constraint (2) is satisfied.[7]

## V. The PMF of Delay

The previous sections discussed our buffer-aided channel selection scheme, which reduces the end-to-end energy dissipation. However, the cost of saving energy is that of having a higher end-to-end packet delay. To analyze the behaviour of the system, we have to study both the average packet delay and the distribution of packet delay. In this section, we first restate the concept of *State* defined in our previous papers [9], [10], [27]. Then, a specific Markov State Transition Matrix (MSTM) is designed. Finally, an algorithm is provided for finding the Probability Mass Function (PMF) of the packet delay.

### A. The Concept of State

The concept of State in buffer-aided systems was proposed in [9], [10]. Upon assuming that the buffer size of the RN is $B$ packets, the state is defined as $S_b = b$, when $b$ packets are stored in the RN. Therefore, the total number of states is $(B+1)$. Given $(B+1)$ states, a state transition matrix denoted by $T$ can be populated by the state transition probabilities $\{T_{i,j} = P(s(t+1) = S_j | s(t) = S_i), i, j = 0, 1, \ldots, B\}$. Let us now find the elements of the MSTM $T$.

### B. The State Transition Matrix T

Based on our discussions in Sections IV-B, the activation probability of each hop is known, when all three channels are available. However, the activation criterion is unknown, when the buffer is either empty or full at the RN. Since this activation criterion does not affect the energy dissipation and outage prediction bound, the system will activate the specific channel having the highest instantaneous SNR amongst the available channels. For example, a state transition matrix associated with $B = 4$ is given below,

$$T = \begin{bmatrix} 1-P_{0,1} & P_{0,1} & 0 & 0 & 0 \\ P_{RD} & P_{SD}+P_{out} & P_{SR} & 0 & 0 \\ 0 & P_{RD} & P_{SD}+P_{out} & P_{SR} & 0 \\ 0 & 0 & P_{RD} & P_{SD}+P_{out} & P_{SR} \\ 0 & 0 & 0 & P_{B,B-1} & 1-P_{B,B-1} \end{bmatrix}. \tag{38}$$

The probability $P_{0,1}$ is represented by the region XDCF+FGU in Fig. 4, yielding

$$P_{0,1} = \left(1 - e^{-\gamma_{SD}^{out}}\right) e^{-\gamma_{SR}^{out}} + P_{SR\{SR\ SD\}} / \left(1 - e^{-\gamma_{RD}^{out}}\right), \tag{39}$$

where $P_{SR\{SR\ SD\}}$ is from (25), while $P_{B,B-1}$ is given by

$$P_{B,B-1} = \left(1 - e^{-\gamma_{SD}^{out}}\right) e^{-\gamma_{RD}^{out}} + P_{RD\{RD\ SD\}} / \left(1 - e^{-\gamma_{SR}^{out}}\right), \tag{40}$$

where $P_{RD\{RD\ SD\}}$ is from (55). If the SD hop is activated or a system outage occurs, the system's state remains unchanged. Therefore the values on the diagonal of $T$ are $(1-P_{0,1})$, $(P_{SD}+P_{out})$ and $(1-P_{B,B-1})$.

Having obtained the MSTM $T$, the steady-state transition probabilities may be computed as follows [8]:

$$\pi(B) = T^T \pi(B), \tag{41}$$

where we have $\pi(B) = [\pi_0, \pi_1, \ldots, \pi_B]^T$ and $\pi_i$ is the steady-state probability of the state $S_i$ [8]. The steady-state probability of a state is the expected probability of this specific state of the system, where (41) shows that $\pi(B)$ is the right eigenvector of the matrix $T^T$ corresponding to an eigenvalue of one. Therefore, $\pi(B)$ can be derived with the aid of classic methods conceived for solving the corresponding eigenvalue problem [30].

### C. An Algorithm for Determining the PMF of Packet Delay

Having determined $\pi(B)$ and $T$, let us now find the PMF of the delay. Let $P_d(t)$ represent the probability of a specific end-to-end packet delay of $t$ TSs. The probability $P_d(1)$ of direct transmission from the SN to DN can be described mathematically, as discussed below.

If a packet is transmitted directly from the SN to DN, the delay of this packet is 1 TS. Then $P_d(1)$ is the ratio of the probability $P_{1TS}^{suc}$ of the packet being successfully transmitted in 1 TS and of the probability of the packet being entered into the buffer-aided queuing system, yielding

$$P_{1TS}^{suc} = \pi_0 \left[1 - P_{0,1} - \left(1 - e^{-\gamma_{SR}^{out}}\right)\left(1 - e^{-\gamma_{SD}^{out}}\right)\right] + \sum_{i=1}^{B-1} \pi_i P_{SD} + \pi_B \left[1 - P_{B,B-1} - \left(1 - e^{-\gamma_{RD}^{out}}\right)\left(1 - e^{-\gamma_{SD}^{out}}\right)\right], \tag{42}$$

[7]The software that can be used for evaluating the results of this paper was uploaded for public use at [28], which may benefit the readers.

where $(1-e^{-\gamma_{SR}^{out}})(1-e^{-\gamma_{SD}^{out}})$ and $(1-e^{-\gamma_{RD}^{out}})(1-e^{-\gamma_{SD}^{out}})$ in the first and last terms represent the outage probability. Therefore, we have:

$$P_d(1)=\frac{P_{1TS}^{suc}}{P_{1TS}^{suc}+\pi_0 P_{0,1}+\sum_{i=1}^{B-1}\pi_i P_{SR}}, \tag{43}$$

where $\pi_0 P_{0,1}+\sum_{i=1}^{B-1}\pi_i P_{sr}$ is the probability of the packet entering the RN's buffer-aided queue.

Having determined $P_d(1)$, let us now find $P_d(i)$, $i>1$ by applying an algorithm similar to that proposed in [31]. We assumed that a so-called test packet is available at the SN when $t=0$. Then we can find the probability $P_d(i), i=2,3,\cdots,\infty$ upon detecting that the test packet arrived at the DN, when we have $t=i\,TS$. For the details, please refer to [31].

With the aid of the PMF of the delay $P_d(t)$, which is the probability of the packet delay being $t$ TSs, the average packet delay $\bar{\tau}$ may be then expressed as

$$\bar{\tau}=\sum_{t=1}^{\infty}P_d(t)\cdot t. \tag{44}$$

An alternative method is based on Little's Law as in [25]. The average delay is

$$\bar{\tau}=1+\frac{\sum_{i=1}^{B}\pi_i i}{P_{1TS}^{suc}+\pi_0 P_{0,1}+\sum_{i=1}^{B-1}\pi_i P_{SR}}, \tag{45}$$

where $\sum_{i=1}^{B}\pi_i i$ represents the total number of packets stored in the buffer, while $P_{1TS}^{suc}+\pi_0 P_{0,1}+\sum_{i=1}^{B-1}\pi_i P_{SR}$ is the denominator of (57).

## VI. Exact OP and End-to-End PED

The concept of state was defined in Section V-A, while the probability of maintaining steady-state operation was obtained in (41). The exact OP and end-to-end PED may be expressed based on our results provided in Section V.

### A. Exact OP

The exact OP is given by the sum of three scenarios of the system state. 1) When the buffer is empty, only the SN-DN and SN-RN channels should be considered. The probability of this case is $\pi_0$ and the corresponding outage probability is $\pi_0(1-e^{-\gamma_{SD}^{out}})(1-e^{-\gamma_{SR}^{out}})$. 2) When the buffer is full, only the SN-DN and RN-DN channels should be considered. The probability of this scenario is $\pi_B$ and the corresponding outage probability is $\pi_B(1-e^{-\gamma_{SD}^{out}})(1-e^{-\gamma_{RD}^{out}})$. 3) Finally, when the buffer is neither empty nor full, all channels should be considered. The probability of this case is $\sum_{i=1}^{B-1}\pi_i$ and the corresponding outage probability is $\sum_{i=1}^{B-1}\pi_i P_{out}$, where $P_{out}$ is from (9). Upon summing these three contributions, the exact OP of a specific buffer size $B$ $[P_{out}(B)]$ becomes

$$P_{out}(B)=\pi_0\left(1-e^{-\gamma_{SD}^{out}}\right)\left(1-e^{-\gamma_{SR}^{out}}\right)+\pi_B\left(1-e^{-\gamma_{SD}^{out}}\right)\left(1-e^{-\gamma_{RD}^{out}}\right)+\sum_{i=1}^{B-1}\pi_i P_{out}. \tag{46}$$

### B. Exact End-to-End PED

Finding the exact end-to-end PED may be a little complex, because the availability of a channel is affected both by the channel SNR as well as by the buffer-fullness. In line with Section VI-A, the exact end-to-end PED is based on the sum of the PED in three specific scenarios of the system state.

1) Firstly, when the buffer is neither empty nor full, all channels should be considered. The probability of this case is $\sum_{i=1}^{B-1}\pi_i$ and the corresponding energy dissipation is $\sum_{i=1}^{B-1}\pi_i(\mathcal{E}_{SR}+\mathcal{E}_{RD}+\mathcal{E}_{SD})$.
2) When the buffer is empty, only the SN-DN and SN-RN channels should be considered. The probability of this case is $\pi_0$. 2-1) If the SR link is activated in the case of $\gamma_{SR}\geq\gamma_{SR}^{out}$ and $\gamma_{SD}<\gamma_{SD}^{out}$, the corresponding energy dissipation is $\mathcal{E}_{SR\{SR\}}/(1-e^{-\gamma_{SD}^{out}})/(1-e^{-\gamma_{RD}^{out}})$, where the term $(1-e^{-\gamma_{SD}^{out}})(1-e^{-\gamma_{RD}^{out}})$ was already taken into account in the calculation of $\mathcal{E}_{SR\{SR\}}$, hence it should be removed. 2-2) By contrast, if the SR link is activated in the case of $\gamma_{SR}\geq\gamma_{SR}^{out}$ and $\gamma_{SD}\geq\gamma_{SD}^{out}$, the corresponding energy dissipation becomes $\mathcal{E}_{SR\{SR\,SD\}}/(1-e^{-\gamma_{RD}^{out}})$ and the associated energy dissipation is $\pi_0(\mathcal{E}_{SR\{SR\}}/(1-e^{-\gamma_{SD}^{out}})+\mathcal{E}_{SR\{SR\,SD\}}+\mathcal{E}_{SD\{SD\}}/(1-e^{-\gamma_{SR}^{out}})+\mathcal{E}_{SD\{SR\,SD\}})/(1-e^{-\gamma_{RD}^{out}})$. 2-3) Similar to case 2-1), if the SD link is activated in the case of $\gamma_{SD}\geq\gamma_{SD}^{out}$ and $\gamma_{SR}<\gamma_{SR}^{out}$, the corresponding energy dissipation becomes $\mathcal{E}_{SD\{SD\}}/(1-e^{-\gamma_{SR}^{out}})/(1-e^{-\gamma_{RD}^{out}})$. 2-4) Finally, if the SD link is activated in the case of $\gamma_{SD}\geq\gamma_{SD}^{out}$ and $\gamma_{SR}\geq\gamma_{SR}^{out}$, the corresponding energy dissipation is $\mathcal{E}_{SD\{SR\,SD\}}/(1-e^{-\gamma_{RD}^{out}})$. The sum of the above four cases multiplied by the probability $\pi_0$ of having an empty buffer is the energy dissipation, yielding

$$\pi_0\left(\mathcal{E}_{SR\{SR\}}/(1-e^{-\gamma_{SD}^{out}})+\mathcal{E}_{SR\{SR\,SD\}}+\mathcal{E}_{SD\{SD\}}/(1-e^{-\gamma_{SR}^{out}})+\mathcal{E}_{SD\{SR\,SD\}}\right)/(1-e^{-\gamma_{RD}^{out}}). \tag{47}$$

3) When the buffer is full, only the SN-DN and RN-DN channels should be considered. The probability of this scenario is $\pi_B$. Based on the same process, the energy dissipation associated with a full buffer may be found. This simply requires substituting RD for SR and the subscript B for 0 in (47).

Therefore, the total energy dissipation $\mathcal{E}(B)$ (in a unit time) associated with a specific buffer size B is

$$\begin{aligned}\mathcal{E}(B)=&\pi_0\left(\mathcal{E}_{SR\{SR\}}/(1-e^{-\gamma_{SD}^{out}})+\mathcal{E}_{SR\{SR\,SD\}}+\mathcal{E}_{SD\{SD\}}/(1-e^{-\gamma_{SR}^{out}})+\mathcal{E}_{SD\{SR\,SD\}}\right)/(1-e^{-\gamma_{RD}^{out}})\\&+\pi_B\left(\mathcal{E}_{RD\{RD\}}/(1-e^{-\gamma_{SD}^{out}})+\mathcal{E}_{RD\{RD\,SD\}}+\mathcal{E}_{SD\{SD\}}/(1-e^{-\gamma_{RD}^{out}})+\mathcal{E}_{SD\{RD\,SD\}}\right)/(1-e^{-\gamma_{SR}^{out}})\\&+\sum_{i=1}^{B-1}\pi_i(\mathcal{E}_{SR}+\mathcal{E}_{RD}+\mathcal{E}_{SD}).\end{aligned} \tag{48}$$

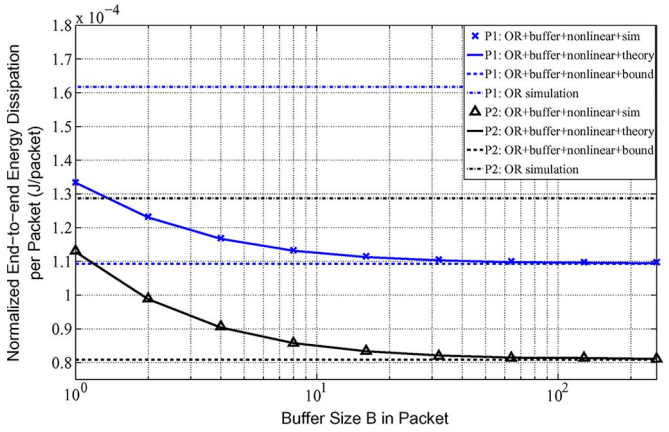


Fig. 5. Average normalized end-to-end energy dissipation per packet as defined in Section III-B when the RN is at the position of (400, 400) and the pathloss factor is $\alpha = 2$. The theoretical curve was evaluated from (36).

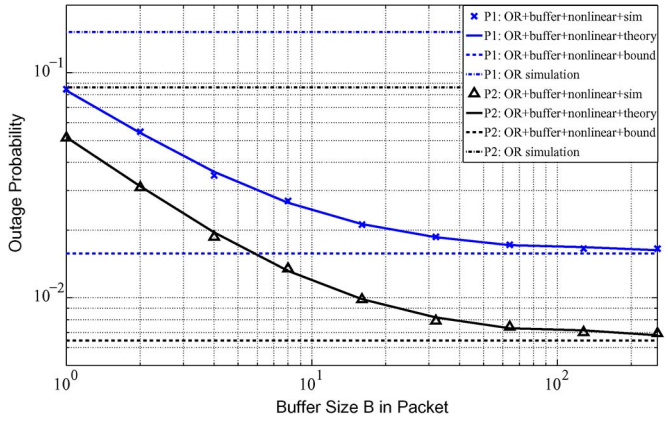


Fig. 6. The simulated and theoretical outage probability evaluated from (9) when the RN is at the position of (400, 400).

The end-to-end throughput may be found based on (48) by changing all variables $\mathcal{E}$ to $P$ and halving all items related to the SR and RN hops. The end-to-end throughput $\Phi(B)$ with a specific buffer size B is

$$\Phi(B) = \pi_0 \Bigg( \frac{1}{2} P_{SR\{SR\}} / (1 - e^{-\gamma_{SD}^{out}}) + \frac{1}{2} P_{SR\{SR\ SD\}} + P_{SD\{SD\}} / (1 - e^{-\gamma_{SR}^{out}}) + P_{SD\{SR\ SD\}} \Bigg) / (1 - e^{-\gamma_{RD}^{out}}) + \pi_B \Bigg( \frac{1}{2} P_{RD\{RD\}} / (1 - e^{-\gamma_{SD}^{out}}) + \frac{1}{2} P_{RD\{RD\ SD\}} + P_{SD\{SD\}} / (1 - e^{-\gamma_{RD}^{out}}) + P_{SD\{RD\ SD\}} \Bigg) / (1 - e^{-\gamma_{SR}^{out}}) + \sum_{i=1}^{B-1} \pi_i \left( \frac{1}{2} P_{SR} + \frac{1}{2} P_{RD} + P_{SD} \right). \quad (49)$$

Finally, the end-to-end PED $\bar{\mathcal{E}}(B)$ for a specific buffer size B is the ratio of the total energy dissipation to the end-to-end throughput, which is

$$\bar{\mathcal{E}}(B) = \frac{\mathcal{E}(B)}{\Phi(B)}. \quad (50)$$

## VII. Performance Results

In this section, we provide a range of numerical and/or simulation results for characterizing the energy dissipation, the OP and the delay of the B3NN considered, to illustrate the effects of both the position of the RN and of the buffer size $B$ of the RN. In all experiments, the SN is at the position (0, 0), while DN is at the position (1000 m, 0). Again, the parameters of $N$ and $\kappa$ are $N = 10^{-14}$ and $\kappa = 9.895 \times 10^{-05}$. The pathloss factor $\alpha$ and the maximum transmit power are $\alpha = 2$ and $P_{max} = 0.0003$ Watt in Figs. 5–9. For convenience, "normalized energy dissipation" refers to the "average normalized end-to-end energy dissipation per packet," which is the optimization objective of this paper.

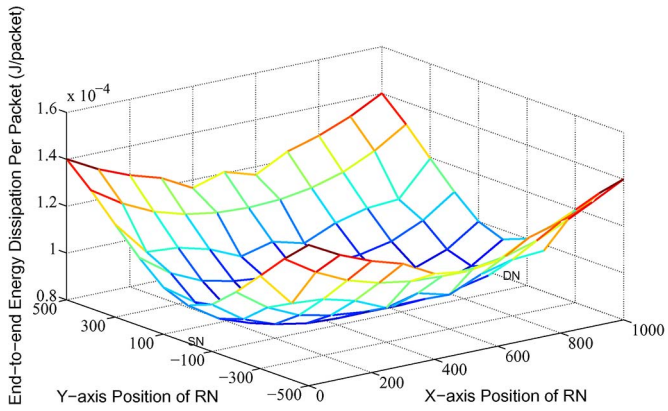


Fig. 7. Average normalized end-to-end energy dissipation vs the RN position. The results are theoretical analysis with assuming of infinity buffer size.

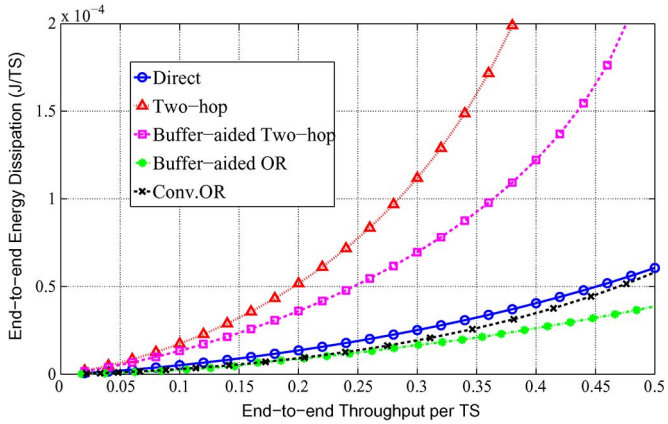


Fig. 8. The end-to-end (system) energy dissipation per TS for various transmission schemes operated at a given target end-to-end throughput where the RN is at the position of (400, 400).

The first set of results characterizes the impact of the RN's buffer size on the end-to-end normalized energy dissipation and the OP. The results of Figs. 5 and 6 are plotted against the buffer size. In both figures, the RN is at the position $P1$: (400, 400) or $P2$: (500, 0), while the buffer size ranges from $B = 1$ to $B = 256$ packets. In Sections III–IV-B3, we discussed the proposed nonlinear channel space partitioning method, its

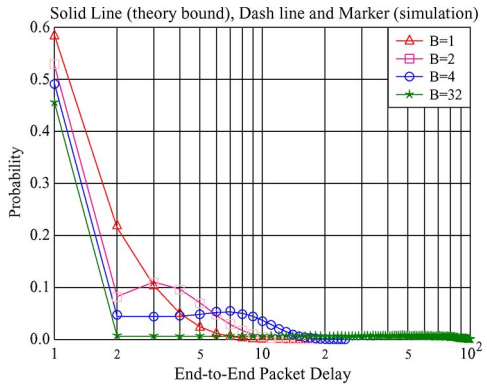


Fig. 9. The distribution of the packet delay evaluated from Section V, when the RN is at the position of (400, 400). The buffer size ranges from 1 to 32.

parameters and the associated theoretical bound (dashed line). Given the principle encapsulated in (8), the analysis of our nonlinear channel space partitioning method can be carried out. The simulation results and the corresponding theoretical results are represented by the solid line marked by a triangle or a cross. The theoretical results associated with a specific buffer size can be obtained by applying the principles detailed in [9] with $\Pi(B)$ from (41). Observe in both Figs. 5 and 6 that the simulation based performance approaches the theoretical energy dissipation bound, as the buffer size increases and that a significant improvement (89.6% for P1) can be achieved over conventional OR [20] (dashed dotted line).

Fig. 7 portrays the normalized energy dissipation versus the position of the RN. This figure applied the same parameters and methodology as those used for Fig. 5, except for the position of the RN. The results are based on our theoretical analysis associated with assuming an infinite buffer size. The positions of both the SN and DN are marked in this figure, while the RN may be located at any position. The normalized energy dissipation can be theoretically calculated from (36), when the RN is in a specific position. Observe in Fig. 7 that the normalized energy dissipation is characterized by a surface as a function of the RN position. Additionally, it is reasonable to expect that the normalized energy dissipation is the lowest, when the RN is in the half-way position between the SN and DN (bottom of the surface), while it is higher, when the RN is far away from both the SN and DN, as indicated by the corners of the surface.

Fig. 8 compares the normalized energy dissipation for various transmission schemes. The RN is at the normalized position of (400, 400) and the pathloss factor is $\alpha = 2$. All results in this figure are theoretical analysis results. The label "Direct" implies that the packet is transmitted directly from the SN to DN without relaying, while the label "Two-hop" means that the packet is transmitted from the SN to DN via the RN sequentially in two hops without buffering. The "Buffer-aided two-hop" scenario implies that the RN has a buffer, therefore the system relies on channel-quality aided activation, however the SN is unable to directly transmit a packet to the DN. This scheme is identical to that proposed in [9]–[11]. The power allocation method mentioned in [32] is applied both in the "Two-hop" scenario and in the "Buffer-aided two-hop" transmission scheme, which makes the average receive SNR for each hop the same. The label "Conv. OR" represents the conventional opportunistic routing method [20], [23], where each packet is transmitted either via the SN-DN or the SN-RN-DN route, one by one. The next packet does not enter the system unless the previous packet has been received by the DN. In other words, the RN is only capable of storing one packet. Finally, the "Buffer-aided OR" is our proposed scheme. The corresponding results are based on our theoretical analysis relying on an infinite buffer size. The X-coordinate represents the end-to-end target throughput, while the Y-coordinate represents the energy dissipation. Observe from Fig. 8 that the performance of both the "Two-hop" and of the "Buffer-aided two-hop" schemes is worse than that of the "Direct" scheme. The "Buffer-aided OR" scheme performs best. The performance of conventional opportunistic routing is worse than that of Buffer-aided OR, but better than that of direct transmission. The reason for this is because compared to direct transmission, conventional OR has more potential routes while in contrast to the buffer-aided OR scheme, conventional OR may only store a single packet in the RN. For example, observe in Fig 8 that when the system is operated at a normalized end-to-end throughput of 0.4 packet/TS, the end-to-end PED of "Buffer-aided OR" was reduced by 88.2%, 77.6%, 32.3% and by 24.8%, when compared to the "Two-hop," "Buffer-aided Two-hop," "Direct" and to the "Conv. OR" transmission schemes, respectively. Compared to the direct transmission scenario, the transmission duration is halved in the "Two-hop" and "Buffer-aided two-hop" scheme. In other words, the target throughput of each hop has to be doubled. This is why those two schemes perform worse. Compared to classic direct transmission, again, the "Buffer-aided OR" scheme is capable of activating the best of the three channels, hence it attains the best performance. Furthermore, the reciprocal of the throughput is related to the average delay, which also shows the advantages of the "Buffer-aided OR" aided transmission scheme.

Fig. 9 shows the distribution of the packet delay, when stipulating the same assumptions, as those for Fig. 5. The theoretical results obtained from Section V are represented by the solid lines, while the simulation results are represented by the markers. It is clear from Fig. 9 that the probability of direct transmission associated with $B = 1$ is relatively high. As shown in Fig. 9, when the buffer size $B$ increases, the probability of direct transmission decays below that of buffer-aided OR.

## VIII. Conclusion

In this contribution, we have proposed and investigated a new routing scheme, which we referred to as the BOR regime that was capable of combining the advantages of buffer-aided transmissions with the benefits of opportunistic routing. Additionally, a specific MAC layer protocol was designed for supporting the proposed BOR. Moreover, a three-dimensional channel space partitioning method was proposed and discussed. Finally, the normalized energy dissipation, the outage probability and the distribution of the delay have been analyzed and a range of formulas have been obtained, when assuming that the packets can be correctly received provided that the received SNR was in excess of a certain threshold. All hops experienced

Rayleigh fading. Our analysis and performance results showed that exploiting the BOR scheme results in a significant reduction of the energy dissipation. The results also show that the theoretical energy dissipation and the outage probability bound can be approached by employing a sufficiently large buffer at the RN. Our future research will consider the benefits of channel space partitioning in multi-hop links.

## APPENDIX

### A. B3NN MAC Protocol

Again, we assume that every node has the global channel quality knowledge and the BF knowledge of the RNs. This facilitates the decisions as to which of the nodes is allowed to transmit. In practice, however, it is a challenge to realize this idealized assumption. Therefore, we have to design protocols for efficiently exchanging the related information, so that the specific hop requiring the least "resources" is activated.

In a new TS, we assume that none of the nodes has any channel quality knowledge or non-local BF knowledge. The operations have three stages. 1) The channel quality of the adjacent nodes is measured first. 2) Then the RN obtain the channel quality of the SN-DN channel. 3) Finally, the RN broadcasts its decision. To elaborate a little further, the operations associated with the above-mentioned three stages are described as follows.

*Stage 1—Channel State Identification:* This stage requires three symbol durations in which the SN, RN and DN broadcast their pilot signals. Upon receiving the pilot signal, the receiver node estimates the corresponding channel quality.

*Stage 2—Disseminate the Remaining Channel Quality Information:* Following ***Stage 1***, every node becomes aware of the channel qualities of the pair of links connected to itself. For example, the SN is informed of the SN-RN and SN-DN link qualities. However, the RN also needs the channel quality of the SN-DN link for deciding upon which of the channels will be activated. To satisfy this requirement, this stage needs another symbol duration. Accordingly, in the 4th symbol duration, the SN broadcasts $\frac{\gamma_{SD}}{h_{SR}}$. Hence, the RN receives $\frac{\gamma_{SD}}{h_{SR}} h_{SR} = \gamma_{SD}$.

*Stage 3—The Decision Carried Out by the RN:* Following ***Stage 1*** and ***Stage 2***, the RN becomes aware of all the channel quality and BF knowledge. Based on this knowledge, the RN decides which particular channel will be activated and broadcasts this decision to the SN and DN. This step requires two more symbol durations.

Following these three stages, the communications may be established. We now formulate a procedure to be applied at the RN and discussed it in the context of our idealized simplifying assumptions.

### B. Determination of $P_{SD\{SD\ RD\}}$ and $P_{RD\{SD\ RD\}}$

The related formulas of $P_{SD\{SD\ RD\}}$ and $P_{RD\{SD\ RD\}}$ are similar to those of $P_{SD\{SD\ SR\}}$ and $P_{SR\{SD\ SR\}}$, which are derived by replacing RD by SR, yielding:

$$\gamma_{SD\{RD\ SD\}} = f_{\{RD->SD\}}\left(\gamma_{RD\{RD\ SD\}}\right) \tag{51}$$

$$= \frac{\gamma_{T_h} d_{SD}^{\alpha} \kappa}{-E_{ffe}\kappa + \bar{\mathcal{E}}_{SR}\kappa + \frac{\gamma_{T_h} d_{RD}^{\alpha} N}{\gamma_{RD\{RD\ SD\}}}}. \tag{52}$$

The domain of definition for $\gamma_{RD\{RD\ SD\}}$ is $(\gamma_{RD\{RD\ SD\}}^{min}, \gamma_{RD\{RD\ SD\}}^{max})$, yielding

$$\gamma_{RD\{RD\ SD\}}^{min} = \max\left\{\gamma_{RD}^{out}, f_{\{RD->SD\}}^{-1}\left(\gamma_{SD}^{out}\right)\right\} \tag{53}$$

$$\gamma_{RD\{RD\ SD\}}^{max} = \begin{cases} \frac{\gamma_{T_h} d_{RD}^{\alpha} N}{E_{ffe}\kappa - \bar{\mathcal{E}}_{SR}\kappa}, & E_{ffe} > \bar{\mathcal{E}}_{SR} \\ \infty, & \text{otherwise.} \end{cases} \tag{54}$$

The activation probability $P_{RD\{RD\ SD\}}$ of the RD link associated with $\gamma_{RD\{RD\ SD\}}$. $P_{RD\{RD\ SD\}}$ is expressed as

$$\begin{aligned} &P_{RD\{RD\ SD\}} \\ &= \left(1 - e^{-\gamma_{SR}^{out}}\right) \int_{\gamma_{RD\{RD\ SD\}}^{min}}^{\gamma_{RD\{RD\ SD\}}^{max}} \mathcal{F}_1\left(\gamma_{RD\{RD\ SD\}}\right) e^{-\gamma_{RD\{RD\ SD\}}} \\ &\quad \times \int_{\gamma_{SD}^{out}}^{f_{\{RD->SD\}}\left(\gamma_{RD\{RD\ SD\}}\right)} e^{-\gamma_{SD\{RD\ SD\}}} \\ &\quad \times d\gamma_{SD\{RD\ SD\}} d\gamma_{RD\{RD\ SD\}} \\ &\quad + \left(1 - e^{-\gamma_{SR}^{out}}\right) e^{-\gamma_{SD}^{out}} \int_{\gamma_{RD\{RD\ SD\}}^{max}}^{\infty} \mathcal{F}_1\left(\gamma_{RD\{RD\ SD\}}\right) \\ &\quad \times e^{-\gamma_{RD\{RD\ SD\}}} d\gamma_{RD\{RD\ SD\}}, \end{aligned} \tag{55}$$

where we have:

$$\gamma_{RD\{RD\ SD\}} = f_{\{SD->RD\}}\left(\gamma_{SD\{RD\ SD\}}\right) \tag{56}$$

$$= \frac{\gamma_{T_h} d_{RD}^{\alpha} \kappa}{E_{ffe}\kappa - \bar{\mathcal{E}}_{SR}\kappa + \frac{\gamma_{T_h} d_{SD}^{\alpha} N}{\gamma_{SD\{RD\ SD\}}}}. \tag{57}$$

The domain of definition for $\gamma_{SD\{RD\ SD\}}$ is $(\gamma_{SD\{RD\ SD\}}^{min}, \gamma_{SD\{RD\ SD\}}^{max})$, yielding

$$\gamma_{SD\{RD\ SD\}}^{min} = \max\left\{\gamma_{SD}^{out}, f_{\{SD->RD\}}^{-1}\left(\gamma_{RD}^{out}\right)\right\} \tag{58}$$

$$\gamma_{SD\{RD\ SD\}}^{max} = \begin{cases} \frac{\gamma_{T_h} d_{SD}^{\alpha} N}{-E_{ffe}\kappa + \bar{\mathcal{E}}_{SR}\kappa}, & E_{ffe} < \bar{\mathcal{E}}_{SR} \\ \infty, & \text{otherwise.} \end{cases} \tag{59}$$

The activation probability $P_{SD\{RD\ SD\}}$ of the SD link associated with $\gamma_{SD\{RD\ SD\}}$, is formulated as:

$$\begin{aligned} &P_{SD\{RD\ SD\}} \\ &= \left(1 - e^{-\gamma_{SR}^{out}}\right) \int_{\gamma_{SD\{RD\ SD\}}^{min}}^{\gamma_{SD\{RD\ SD\}}^{max}} \mathcal{F}_1\left(\gamma_{SD\{RD\ SD\}}\right) \\ &\quad \times e^{-\gamma_{SD\{RD\ SD\}}} \\ &\quad \times \int_{\gamma_{RD}^{out}}^{f_{\{SD->RD\}}\left(\gamma_{SD\{RD\ SD\}}\right)} e^{-\gamma_{RD\{RD\ SD\}}} \\ &\quad \times d\gamma_{RD\{RD\ SD\}} d\gamma_{SD\{RD\ SD\}} \\ &\quad + \left(1 - e^{-\gamma_{SR}^{out}}\right) e^{-\gamma_{RD}^{out}} \int_{\gamma_{SD\{RD\ SD\}}^{max}}^{\infty} \mathcal{F}_1\left(\gamma_{SD\{RD\ SD\}}\right) \\ &\quad \times e^{-\gamma_{SD\{RD\ SD\}}} d\gamma_{SD\{RD\ SD\}}. \end{aligned} \tag{60}$$

### C. Derivation of $P_{SR\{SR\ RD\}}$ and $P_{RD\{SR\ RD\}}$

Again, the process is the same as before. Note that value of the $E_{ffe}$ is doubled, when changing the region from SR to RD, provided that we have $P_{SR\{SR\ RD\}} > P_{RD\{SR\ RD\}}$, because the assumption without loss of generality in that we have $d_{SR} < d_{RD}$. This yields:

$$\gamma_{SR\{RD\ SR\}} = f_{\{RD->SR\}}\left(\gamma_{RD\{RD\ SR\}}\right) \tag{61}$$

$$= \frac{\gamma_{T_h} d_{SR}^{\alpha} \kappa}{-2E_{ffe}\kappa + (\bar{\mathcal{E}}_{SR} - \bar{\mathcal{E}}_{RD})\kappa + \frac{\gamma_{T_h} d_{RD}^{\alpha} N}{\gamma_{RD\{RD\ SR\}}}}. \tag{62}$$

The domain of definition for $\gamma_{RD\{RD\ SR\}}$ is $(\gamma^{min}_{RD\{RD\ SR\}}, \gamma^{max}_{RD\{RD\ SR\}})$, yielding

$$\gamma^{min}_{RD\{RD\ SR\}} = \max\left\{\gamma^{out}_{RD}, f^{-1}_{\{RD->SR\}}(\gamma^{out}_{SR})\right\} \tag{63}$$

$$\gamma^{max}_{RD\{RD\ SR\}} = \begin{cases} \frac{\gamma_{T_h} d_{RD}^{\alpha} N}{2E_{ffe}\kappa - (\bar{\mathcal{E}}_{SR} - \bar{\mathcal{E}}_{RD})\kappa}, & 2E_{ffe} > (\bar{\mathcal{E}}_{SR} - \bar{\mathcal{E}}_{RD}) \\ \infty, & \text{otherwise.} \end{cases} \tag{64}$$

The activation probability $P_{RD\{RD\ SR\}}$ of the RD link associated with $\gamma_{RD\{RD\ SR\}}$ is formulated as:

$$\begin{aligned} P_{RD\{RD\ SR\}} &= \left(1 - e^{-\gamma^{out}_{SD}}\right) \int_{\gamma^{min}_{RD\{RD\ SR\}}}^{\gamma^{max}_{RD\{RD\ SR\}}} \mathcal{F}_1\left(\gamma_{RD\{RD\ SR\}}\right) \\ &\quad \times e^{-\gamma_{RD\{RD\ SR\}}} \\ &\quad \times \int_{\gamma^{out}_{SR}}^{f_{\{RD->SR\}}\left(\gamma_{RD\{RD\ SR\}}\right)} e^{-\gamma_{SR\{RD\ SR\}}} \\ &\quad \times d\gamma_{SR\{RD\ SR\}} d\gamma_{RD\{RD\ SR\}} \\ &\quad + (1 - e^{-\gamma^{out}_{SD}}) e^{-\gamma^{out}_{SR}} \int_{\gamma^{max}_{RD\{RD\ SR\}}}^{\infty} \mathcal{F}_1\left(\gamma_{RD\{RD\ SR\}}\right) \\ &\quad \times e^{-\gamma_{RD\{RD\ SR\}}} d\gamma_{RD\{RD\ SR\}}, \end{aligned} \tag{65}$$

where

$$\gamma_{RD\{RD\ SR\}} = f_{\{SR->RD\}}\left(\gamma_{SR\{RD\ SR\}}\right) \tag{66}$$

$$= \frac{\gamma_{T_h} d_{RD}^{\alpha} \kappa}{2E_{ffe}\kappa + (\bar{\mathcal{E}}_{RD} - \bar{\mathcal{E}}_{SR})\kappa + \frac{\gamma_{T_h} d_{SD}^{\alpha} N}{\gamma_{SR\{RD\ SR\}}}}. \tag{67}$$

The domain of definition for $\gamma_{SR\{RD\ SR\}}$ is $(\gamma^{min}_{SR\{RD\ SR\}}, \gamma^{max}_{SR\{RD\ SR\}})$, yielding

$$\gamma^{min}_{SR\{RD\ SR\}} = \max\left\{\gamma^{out}_{SR}, f^{-1}_{\{SR->RD\}}(\gamma^{out}_{RD})\right\} \tag{68}$$

$$\gamma^{max}_{SR\{RD\ SR\}} = \begin{cases} \frac{\gamma_{T_h} d_{RD}^{\alpha} N}{-2E_{ffe}\kappa + (\bar{\mathcal{E}}_{SR} - \bar{\mathcal{E}}_{RD})\kappa}, & 2E_{ffe} < (\bar{\mathcal{E}}_{SR} - \bar{\mathcal{E}}_{RD}) \\ \infty, & \text{otherwise.} \end{cases} \tag{69}$$

The activation probability $P_{RD\{RD\ SR\}}$ of the RD link associated with $\gamma_{RD\{RD\ SR\}}$ is given by:

$$\begin{aligned} P_{RD\{RD\ SR\}} &= \left(1 - e^{-\gamma^{out}_{SD}}\right) \int_{\gamma^{min}_{SR\{RD\ SR\}}}^{\gamma^{max}_{SR\{RD\ SR\}}} \mathcal{F}_1\left(\gamma_{SR\{RD\ SR\}}\right) e^{-\gamma_{SR\{RD\ SR\}}} \\ &\quad \times \int_{\gamma^{out}_{RD}}^{f_{\{SR->RD\}}\left(\gamma_{SR\{RD\ SR\}}\right)} e^{-\gamma_{RD\{RD\ SR\}}} \\ &\quad \times d\gamma_{RD\{RD\ SR\}} d\gamma_{SR\{RD\ SR\}} \\ &\quad + \left(1 - e^{-\gamma^{out}_{SD}}\right) e^{-\gamma^{out}_{RD}} \int_{\gamma^{max}_{SR\{RD\ SR\}}}^{\infty} \mathcal{F}_1\left(\gamma_{SR\{RD\ SR\}}\right) \\ &\quad \times e^{-\gamma_{SR\{RD\ SR\}}} d\gamma_{SR\{RD\ SR\}}. \end{aligned} \tag{70}$$

### D. Derivation of $P_{SD\{SD\ SR\ RD\}}$, $P_{SR\{SD\ SR\ RD\}}$, and $P_{RD\{SD\ SR\ RD\}}$

The activation decisions of three channels are more complex than those of two channels, where the latter is associated with the region PKTI of Fig. 3. The calculation of the three-channel system's activation probability relies on our previous results, such as the previous $\gamma^{max}$ and $\gamma^{min}$ results. Based on the specific parameters of $(E_{ffe}, \bar{\mathcal{E}}_{SR}, \bar{\mathcal{E}}_{RD})$, it can be decided whether $\gamma^{max}_{SR\{SR\ RD\}}$ or $\gamma^{max}_{SR\{SR\ SD\}}$ is higher. Let us assume that we have $\gamma^{max}_{SR\{SR\ RD\}} < \gamma^{max}_{SR\{SR\ SD\}}$. Hence the activation probability of the SR hop is formulated as:

$$\begin{aligned} P_{SR\{SR\ SD\ RD\}} &= \int_{\max\{\gamma^{out}_{SR}, \gamma^{min}_{SR\{SR\ RD\}}, \gamma^{min}_{SR\{SR\ SD\}}\}}^{\max\{\gamma^{max}_{SR\{SR\ RD\}}, \gamma^{min}_{SR\{SR\ RD\}}, \gamma^{min}_{SR\{SR\ SD\}}\}} \\ &\quad \times \mathcal{F}_1(\gamma_{SD\{SR\ SD\ RD\}}) e^{-\gamma_{SR\{SR\ SD\ RD\}}} \\ &\quad \times \int_{\gamma^{out}_{RD}}^{f_{\{SR->RD\}}(\gamma_{SR\{SR\ SD\ RD\}})} e^{-\gamma_{RD\{SR\ SD\ RD\}}} \\ &\quad \times \int_{\gamma^{out}_{SD}}^{f_{\{SR->SD\}}(\gamma_{SR\{SR\ SD\ RD\}})} e^{-\gamma_{SD\{SR\ SD\ RD\}}} \\ &\quad \times d\gamma_{SD\{SR\ SD\ RD\}} d\gamma_{RD\{SR\ SD\ RD\}} d\gamma_{SR\{SR\ SD\ RD\}} \\ &\quad + e^{-\gamma^{out}_{RD}} \int_{\max\{\gamma^{out}_{SR}, \gamma^{max}_{SR\{SR\ RD\}}\}}^{\max\{\gamma^{out}_{SR}, \gamma^{max}_{SR\{SR\ SD\}}, \gamma^{min}_{SR\{SR\ SD\}}\}} \\ &\quad \times \mathcal{F}_1(\gamma_{SD\{SR\ SD\ RD\}}) e^{-\gamma_{SR\{SR\ SD\ RD\}}} \\ &\quad \times \int_{\gamma^{out}_{SD}}^{f_{\{SR->SD\}}(\gamma_{SR\{SR\ SD\ RD\}})} e^{-\gamma_{SD\{SR\ SD\ RD\}}} \\ &\quad \times d\gamma_{SD\{SR\ SD\ RD\}} d\gamma_{SR\{SR\ SD\ RD\}} \\ &\quad + e^{-\gamma^{out}_{RD}} e^{-\gamma^{out}_{SD}} \int_{\max\{\gamma^{out}_{SR}, \gamma^{max}_{SR\{SR\ RD\}}\}}^{\infty} \\ &\quad \times \mathcal{F}_1(\gamma_{SD\{SR\ SD\ RD\}}) e^{-\gamma_{SR\{SR\ SD\ RD\}}} \\ &\quad \times d\gamma_{SR\{SR\ SD\ RD\}}. \end{aligned} \tag{71}$$

The relevant formulas may also be readily derived for $\gamma_{SR\{SR\ RD\}}^{max} > \gamma_{SR\{SR\ SD\}}^{max}$. Based on the same process, we may formulate the equations of $P_{RD\{SR\ SD\ RD\}}$ and $P_{SD\{SR\ SD\ RD\}}$, yielding:

$$
\begin{aligned}
&P_{RD\{SR\ SD\ RD\}} \\
&\quad= \int_{\max\{\gamma_{RD}^{out},\gamma_{RD\{SR\ RD\}}^{min},\gamma_{RD\{RD\ SD\}}^{min}\}}^{\max\{\gamma_{RD}^{out},\gamma_{RD\{SR\ SD\}}^{max},\gamma_{RD\{RD\ SD\}}^{min}\}} \\
&\qquad\times \mathcal{F}_1(\gamma_{RD\{SR\ SD\ RD\}}) e^{-\gamma_{RD\{SR\ SD\ RD\}}} \\
&\qquad\times \int_{\gamma_{SD}^{out}}^{f_{\{RD->SD\}}(\gamma_{RD\{SR\ SD\ RD\}})} e^{-\gamma_{SD\{SR\ SD\ RD\}}} \\
&\qquad\times \int_{\gamma_{SR}^{out}}^{f_{\{RD->SR\}}(\gamma_{RD\{SR\ SD\ RD\}})} e^{-\gamma_{SR\{SR\ SD\ RD\}}} \\
&\qquad\times d\gamma_{SR\{SR\ SD\ RD\}} d\gamma_{SD\{SR\ SD\ RD\}} d\gamma_{RD\{SR\ SD\ RD\}} \\
&\qquad+ e^{-\gamma_{SR}^{out}} \int_{\max\{\gamma_{RD}^{out},\gamma_{RD\{SR\ SD\}}^{min},\gamma_{RD\{RD\ SD\}}^{min}\}}^{\max\{\gamma_{RD}^{out},\gamma_{RD\{SR\ RD\}}^{max},\gamma_{RD\{SD\ RD\}}^{max}\}} \\
&\qquad\times \mathcal{F}_1(\gamma_{RD\{SR\ SD\ RD\}}) e^{-\gamma_{RD\{SR\ SD\ RD\}}} \\
&\qquad\times \int_{\gamma_{SD}^{out}}^{f_{\{RD->SD\}}(\gamma_{RD\{SR\ SD\ RD\}})} e^{-\gamma_{SD\{SR\ SD\ RD\}}} \\
&\qquad\times d\gamma_{SD\{SR\ SD\ RD\}} d\gamma_{RD\{SR\ SD\ RD\}} \\
&\qquad+ e^{-\gamma_{SD}^{out}} e^{-\gamma_{SR}^{out}} \int_{\max\{\gamma_{RD}^{out},\gamma_{RD\{SR\ RD\}}^{max},\gamma_{RD\{SD\ RD\}}^{max}\}}^{\infty} \\
&\qquad\times \mathcal{F}_1(\gamma_{RD\{SR\ SD\ RD\}}) e^{-\gamma_{RD\{SR\ SD\ RD\}}} \\
&\qquad\times d\gamma_{RD\{SR\ SD\ RD\}}.
\end{aligned} \tag{72}
$$

$$
\begin{aligned}
&P_{SD\{SR\ SD\ RD\}} \\
&\quad= \int_{\max\{\gamma_{SD}^{out},\gamma_{SD\{SD\ RD\}}^{min},\gamma_{SD\{SD\ SR\}}^{min}\}}^{\max\{\gamma_{SD}^{out},\gamma_{SD\{SR\ SD\}}^{max},\gamma_{SD\{SD\ RD\}}^{min}\}} \\
&\qquad\times \mathcal{F}_1\left(\gamma_{SD\{SR\ SD\ RD\}}\right) e^{-\gamma_{SD\{SR\ SD\ RD\}}} \\
&\qquad\times \int_{\gamma_{RD}^{out}}^{f_{\{SD->RD\}}(\gamma_{SD\{SR\ SD\ RD\}})} e^{-\gamma_{RD\{SR\ SD\ RD\}}} \\
&\qquad\times \int_{\gamma_{SR}^{out}}^{f_{\{SD->SR\}}(\gamma_{SD\{SR\ SD\ RD\}})} e^{-\gamma_{SR\{SR\ SD\ RD\}}} \\
&\qquad\times d\gamma_{SR\{SR\ SD\ RD\}} d\gamma_{RD\{SR\ SD\ RD\}} d\gamma_{SD\{SR\ SD\ RD\}} \\
&\qquad+ e^{-\gamma_{SR}^{out}} \int_{\max\{\gamma_{SD}^{out},\gamma_{SD\{SR\ SD\}}^{max},\gamma_{SD\{SD\ RD\}}^{min}\}}^{\max\{\gamma_{SD}^{out},\gamma_{SD\{SD\ RD\}}^{max}\}} \\
&\qquad\times \mathcal{F}_1(\gamma_{SD\{SR\ SD\ RD\}}) e^{-\gamma_{SD\{SR\ SD\ RD\}}} \\
&\qquad\times \int_{\gamma_{RD}^{out}}^{f_{\{SD->RD\}}(\gamma_{SD\{SR\ SD\ RD\}})} e^{-\gamma_{RD\{SR\ SD\ RD\}}} \\
&\qquad\times d\gamma_{RD\{SR\ SD\ RD\}} d\gamma_{SD\{SR\ SD\ RD\}} \\
&\qquad+ e^{-\gamma_{RD}^{out}} e^{-\gamma_{SR}^{out}} \int_{\max\{\gamma_{SD}^{out},\gamma_{SD\{SD\ RD\}}^{max}\}}^{\infty} \\
&\qquad\times \mathcal{F}_1(\gamma_{SD\{SR\ SD\ RD\}}) e^{-\gamma_{SD\{SR\ SD\ RD\}}} \\
&\qquad\times d\gamma_{SD\{SR\ SD\ RD\}},
\end{aligned} \tag{73}
$$

where we assumed that $\gamma_{SD\{SD\ SR\}}^{max} < \gamma_{SD\{SD\ RD\}}^{max}$.

## REFERENCES


[1] M. O. Hasna and M.-S. Alouini, "Harmonic mean and end-to-end performance of transmission systems with relays," *IEEE Trans. Commun.*, vol. 52, no. 1, pp. 130–135, Jan. 2004.

[2] H.-C. Yang, N. Belhaj, and M.-S. Alouini, "Performance analysis of joint adaptive modulation and diversity combining over fading channels," *IEEE Trans. Commun.*, vol. 55, no. 3, pp. 520–528, Mar. 2007.

[3] M. Mardani, J. S. Harsini, F. Lahouti, and B. Eliasi, "Joint adaptive modulation-coding and cooperative ARQ for wireless relay networks," in *Proc. IEEE ISWCS*, Reykjavik, Iceland, Oct. 2008, pp. 319–323.

[4] D. Wubben, "High quality end-to-end-link performance," *IEEE Veh. Technol. Mag.*, vol. 4, no. 3, pp. 26–32, Sep. 2009.

[5] A. Muller and H.-C. Yang, "Dual-hop adaptive packet transmission systems with regenerative relaying," *IEEE Trans. Wireless Commun.*, vol. 9, no. 1, pp. 234–244, Jan. 2010.

[6] F. A. Onat *et al.*, "Threshold selection for SNR-based selective digital relaying in cooperative wireless networks," *IEEE Trans. Wireless Commun.*, vol. 7, no. 11, pp. 4226–4237, Nov. 2008.

[7] B. Xia, Y. Fan, J. S. Thompson, and H. V. Poor, "Buffering in a three-node relay network," *IEEE Trans. Wireless Commun.*, vol. 7, no. 11, pp. 4492–4496, Nov. 2008.

[8] Z. Lin, E. Erkip, and M. Ghosh, "Rate adaptation for cooperative systems," in *Proc. IEEE GLOBECOM*, San Francisco, CA, USA, Dec. 2006, pp. 1–5.

[9] C. Dong, L.-L. Yang, and L. Hanzo, "Performance analysis of multi-hop diversity aided multi-hop links," *IEEE Trans. Veh. Technol.*, vol. 61, no. 6, pp. 2504–2516, Jul. 2012.

[10] L.-L. Yang, C. Dong, and L. Hanzo, "Multihop diversity-a precious source of fading mitigation in multihop wireless networks," in *Proc. IEEE GLOBECOM*, Houston, TX, USA, Dec. 2011, pp. 1–5.

[11] C. Dong, L.-L. Yang, and L. Hanzo, "Multihop diversity for fading mitigation in multihop wireless networks," in *Proc. IEEE VTC-Fall*, San Francisco, CA, USA, Sep. 2011, pp. 1–5.

[12] A. Ikhlef, D. S. Michalopoulos, and R. Schober, "Max-max relay selection for relays with buffers," *IEEE Trans. Wireless Commun.*, vol. 11, no. 3, pp. 1124–1135, Mar. 2012.

[13] A. Ikhlef, J. Kim, and R. Schober, "Mimicking full-duplex relaying using half-duplex relays with buffers," *IEEE Trans. Veh. Technol.*, vol. 61, no. 7, pp. 3025–3037, Sep. 2012.

[14] G. Chen, Z. Tian, Y. Gong, and J. Chambers, "Decode-and-forward buffer-aided relay selection in cognitive relay networks," *IEEE Trans. Veh. Technol.*, vol. 63, no. 9, pp. 4723–4728, Nov. 2014.

[15] Z. Tian, G. Chen, Y. Gong, Z. Chen, and J. Chambers, "Buffer-aided max-link relay selection in amplify-and-forward cooperative networks," *IEEE Trans. Veh. Technol.*, vol. 64, no. 2, pp. 553–565, Feb. 2015.

[16] G. Chen, Z. Tian, Y. Gong, Z. Chen, and J. Chambers, "Max-ratio relay selection in secure buffer-aided cooperative wireless networks," *IEEE Trans. Inf. Forensics Security*, vol. 9, no. 4, pp. 719–729, Apr. 2014.

[17] N. Zlatanov and R. Schober, "Buffer-aided relaying with adaptive link selection-fixed and mixed rate transmission," *IEEE Trans. Inf. Theory*, vol. 59, no. 5, pp. 2816–2840, May 2013.

[18] T. Islam, A. Ikhlef, R. Schober, and V. K. Bhargava, "Diversity and delay analysis of buffer-aided {BICM-OFDM} relaying," *IEEE Trans. Wireless Commun.*, vol. 12, no. 11, pp. 5506–5519, Nov. 2013.

[19] J. N. Laneman, D. N. Tse, and G. W. Wornell, "Cooperative diversity in wireless networks: Efficient protocols and outage behavior," *IEEE Trans. Inf. Theory*, vol. 50, no. 12, pp. 3062–3080, Dec. 2004.

[20] S. Biswas and R. Morris, "ExOR: Opportunistic multi-hop routing for wireless networks," in *Proc. ACM SIGCOMM*, Philadelphia, PA, USA, Aug. 2005, pp. 133–144.

[21] H. Liu, B. Zhang, H. Mouftah, X. Shen, and J. Ma, "Opportunistic routing for wireless Ad Hoc and sensor networks: Present and future directions," *IEEE Commun. Mag.*, vol. 47, no. 12, pp. 103–109, Dec. 2009.

[22] K. Zeng, Z. Yang, and W. Lou, "Location-aided opportunistic forwarding in multirate and multihop wireless networks," *IEEE Trans. Veh. Technol.*, vol. 58, no. 6, pp. 3032–3040, Jul. 2009.

[23] J. Zuo *et al.*, "Cross-layer aided energy-efficient opportunistic routing in ad hoc networks," *IEEE Trans. Commun.*, vol. 62, no. 2, pp. 522–535, Feb. 2014.

[24] N. Zlatanov, R. Schober, and P. Popovski, "Buffer-aided relaying with adaptive link selection," *IEEE J. Sel. Areas Commun.*, vol. 31, no. 8, pp. 1530–1542, Aug. 2013.

[25] N. C. Beaulieu and J. Hu, "A closed-form expression for the outage probability of decode-and-forward relaying in dissimilar Rayleigh fading channels," *IEEE Commun. Lett.*, vol. 10, no. 12, pp. 813–815, Dec. 2006.

[26] I. Gradshteyn and I. Ryzhik, *Table of Integrals, Series, Products, Seventh Edition*. Amsterdam, The Netherlands: Elsevier, 2007.
[27] I. Krikidis, T. Charalambous, and J. Thompson, "Buffer-aided relay selection for cooperative diversity systems without delay constraints," *IEEE Trans. Wireless Commun.*, vol. 11, no. 5, pp. 1957–1967, May 2012.
[28] C. Dong, L.-L. Yang, J. Zuo, S. X. Ng, and L. Hanzo, *Energy, Delay and Outage Analysis of a Buffer-Aided Three-Node Network Relying on Opportunistic Routing*. [Online]. Available: http://eprints.soton.ac.uk/350501/
[29] R. Horn and C. Johnson, *Matrix Analysis*. New York, NY, USA: Cambridge Univ. Press, Apr. 1986.
[30] C. Dong, L.-L. Yang, and L. Hanzo, "Performance of buffer-aided adaptive modulation in multihop communications," *IEEE Trans. Commun.* [Online]. Available: http://eprints.soton.ac.uk/348686/
[31] C. Dong, L.-L. Yang, and L. Hanzo, "Multi-hop diversity aided multi-hop communications: A cumulative distribution function aware approach," *IEEE Trans. Commun.*, vol. 61, no. 11, pp. 4486–4499, Nov. 2013.

**Chen Dong** received the B.S. degree in electronic information sciences and technology from the University of Science and Technology of China (USTC), Hefei, China, in 2004, the M.Eng. degree in pattern recognition and automatic equipment from the University of Chinese Academy of Sciences, Beijing, China, in 2007, and the Ph.D. degree from the University of Southampton, Southampton, U.K., in 2014, where he is now a Postdoctoral Researcher. He was the recipient of scholarship under the U.K.–China Scholarships for Excellence Programme and has been awarded the Best Paper Award at IEEE VTC 2014-Fall. His research interests include applied math, relay system, channel modelling and cross-layer optimization.

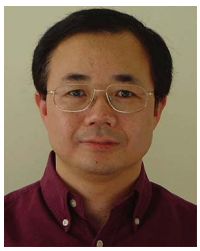

**Lie-Liang Yang** (M'98–SM'02) received the B.Eng. degree in communications engineering from Shanghai TieDao University, Shanghai, China, in 1988, and the M.Eng. and Ph.D. degrees in communications and electronics from Northern (Beijing) Jiaotong University, Beijing, China, in 1991 and 1997, respectively. From June 1997 to December 1997, he was a Visiting Scientist of the Institute of Radio Engineering and Electronics, Academy of Sciences of the Czech Republic. Since December 1997, he has been with the University of Southampton, Southampton, U.K., where he is a Professor of wireless communications in the School of Electronics and Computer Science. Dr. Yang's research has covered a wide range of topics in wireless communications, networking and signal processing. He has published over 300 research papers in journals and conference proceedings, authored/co-authored three books and also published several book chapters. The details about his publications can be found at http://www-mobile.ecs.soton.ac.uk/lly/. He is a Fellow of the IET, served as an associate editor to IEEE TRANSACTIONS ON VEHICULAR TECHNOLOGY and *Journal of Communications and Networks* (JCN), and is currently an Associate Editor to IEEE ACCESS and *Security and Communication Networks (SCN)*.

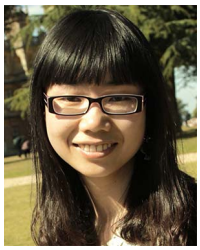

**Jing Zuo** received the B.Eng. degree in communications engineering and the M.Sc. degree in communications and information systems from Jilin University, Changchun, China, in 2006 and 2008, and the Ph.D. degree in wireless communications from University of Southampton, Southampton, U.K., in 2013. She is the recipient of scholarship under the U.K.–China Scholarships for Excellence Programme from 2008 to 2011. From 2009 to 2013, she was involved in the OPTIMIX and CONCERTO European projects. She current works in Huawei, Shenzhen, China and her current research interests include protocols and algorithms design, cross-layer optimization and opportunistic communications.

**Soon Xin Ng** (S'99–M'03–SM'08) received the B.Eng. degree (first class) in electronic engineering and the Ph.D. degree in telecommunications from the University of Southampton, Southampton, U.K., in 1999 and 2002, respectively. From 2003 to 2006, he was a Postdoctoral Research Fellow working on collaborative European research projects known as SCOUT, NEWCOM and PHOENIX. Since August 2006, he has been a member of academic staff in the School of Electronics and Computer Science, University of Southampton. He is involved in the OPTIMIX and CONCERTO European projects as well as the IU-ATC and UC4G projects. He is currently an Associate Professor in telecommunications at the University of Southampton. His research interests include adaptive coded modulation, coded modulation, channel coding, space-time coding, joint source and channel coding, iterative detection, OFDM, MIMO, cooperative communications, distributed coding, quantum error correction codes and joint wireless-and-optical-fiber communications. He has published over 180 papers and co-authored two John Wiley/IEEE Press books in this field. He is a Senior Member of the IEEE, a Chartered Engineer and a Fellow of the Higher Education Academy in the U.K.

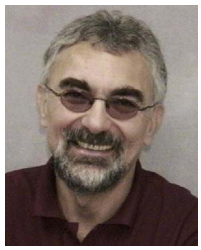

**Lajos Hanzo** received the degree in electronics in 1976 and the doctorate degree in 1983. In 2009, he was awarded the honorary doctorate Doctor Honoris Causa by the Technical University of Budapest. During his 37-year career in telecommunications he has held various research and academic posts in Hungary, Germany and the U.K. Since 1986, he has been with the School of Electronics and Computer Science, University of Southampton, Southampton, U.K., where he holds the chair in telecommunications. He has successfully supervised more than 80+ Ph.D. students, co-authored 20 John Wiley/IEEE Press books on mobile radio communications totalling in excess of 10 000 pages, published 1460 research entries at IEEE Xplore, acted both as TPC and General Chair of IEEE conferences, presented keynote lectures and has been awarded a number of distinctions. Currently he is directing a 60-strong academic research team, working on a range of research projects in the field of wireless multimedia communications sponsored by industry, the Engineering and Physical Sciences Research Council (EPSRC) U.K., the European Research Council's Advanced Fellow Grant and the Royal Society's Wolfson Research Merit Award. He is an enthusiastic supporter of industrial and academic liaison and he offers a range of industrial courses. He is also a Governor of the IEEE VTS. During 2008–2012, he was the Editor-in-Chief of the IEEE Press and a Chaired Professor also at Tsinghua University, Beijing. His research is funded by the European Research Council's Senior Research Fellow Grant. For further information on research in progress and associated publications please refer to http://www-mobile.ecs.soton.ac.uk.